F.E.M. POLYNOMIAL INVERSE ESTIMATES AND ELASTOSTATIC HIGHER ORDER ESTIMATOR

MAHARAVO RANDRIANARIVONY

Abstract. We consider compressible models in computations where higher order Finite Element Method is used. That is, the polynomial degrees are allowed to be arbitrary but fixed over the entire mesh. We treat polynomial inverse estimates and their application to elastostatic a-posteriori error estimators in which inequalities using weighted norms in Sobolev spaces are investigated. Some parameters specify the power of the weights which are generalized Gegenbauer polynomials expressed in term of barycentric coordinates. We report on numerical results related to the strain, stress, displacement and a-posteriori estimates to supplement the theoretical analysis.

1. Introduction

Elastostatic FEM computation occurs in several disciplines comprising CAD integration for structure computation [1] and molecular material design in mesoscale range [12]. We consider the FEM treatment of elastostatic problem governed by the operator

$$-\frac{E}{2(1+\nu)}\Delta\mathbf{U}-\frac{E}{2(1+\nu)(1-2\nu)}\mathbf{grad}(\operatorname{div}\mathbf{U}). \tag{1.1}$$

Apart from faster convergence, the advantage of higher order FEM over the piecewise linear setting is as follows. The elasticity FEM convergence depends on the Young's modulus and Poisson ratio (E,ν) where $\nu<1/2$. When the elastic material approaches incompressibility, i.e. the value of ν is very close to $1/2$, the piecewise linear setting is not guaranteed to converge. That inconvenience is better known as *locking phenomenon* [4, 36]. One popular method of avoiding the locking phenomenon is to increase the polynomial degree when using the displacement formulation. Another technique for circumventing locking is to apply a mixed formulation where the stress tensor is directly used as part of the unknown functions beside an artificial pressure. Anyway, we concentrate in this article on absolutely compressible materials ($\nu\leq\nu_0\ll 1/2$) and we treat polynomial inverse estimates together with their applications to higher order FEM by computing elastostatic simulation. The estimates describe inequalities of polynomials of given degree in term of weighted Sobolev norms. In [19, 20], some such inverse estimates are already documented but they use another type of weights. In effect, their weight function is expressed as the distance to a point with the boundary of a triangle. In contrast, we consider weight functions which are expressed in barycentric

coordinates which make the evaluation computationally efficient. Polynomial inverse estimates are not only important for theoretical purpose. They do also appear in practical application of a-posteriori estimators. In fact, the estimators have to be evaluated in every element of the entire mesh. Thus, in order to compute the APEE in practice, the weight functions need to be evaluated a large number of times. It is therefore important to have a function which is not intensive to evaluate.

Before our exposition, we briefly survey some related works and our previous results. Verfürth has compiled a comprehensive study [33] about APEE (a-posteriori error estimator) for which he mainly treats piecewise linear FEM. Many different a-posteriori error estimators have been proposed for the Stokes problem [34, 35, 2, 14] for isotropic grids. An article [11] by Creusé, Kunert and Nicaise presents a survey on the residual based error estimator on anisotropic grids for the Stokes equation. An interesting APEE for two and three dimensions as well as an anisotropic adaptive mesh refinement are also detailed in [30]. Basically, a-posteriori error estimators permit to evaluate the finite element errors without knowing the exact solution. That feature makes it possible to dynamically identify regions where one should have further refinements [6, 23] if the error there is too large. Therefore, adaptive refinements are mainly based on the quality of a-posteriori error estimators. Our approach in this paper follows the same spirit as the works in [19, 7]. For the Spectral Element Method, we find in [7] an APEE for the *hp*-case which has been generalized in [19] to treat *hp*-FEM [20] for the Poisson problem where corner singularities are allowed. We have presented in [23] an APEE based on hierarchical space enrichment on anisotropic FEM which is combined with adaptive refinements. It is also possible to treat the elasticity problem by using Boundary Element Method (BEM) [15, 29, 28] because the fundamental solution using the Kelvin tensor is available for the Navier-Lamé equation. But we consider in this article FEM which is more standard in both industrial and academic applications. In addition, extending the implementation of the wavelet BEM to elasticity seems to be a lot of work, even with experience on Poisson problem, because it involves vector-valued functions while the single/double layer kernels are matrix-valued. So far, we are not aware of any wavelet BEM which can solve elastostatic problem even on simple models, let alone on real CAD models in a comparable efficiency as FEM (including higher order bases, parallelization and domain decomposition). As far as mesoscale molecular elasticity is concerned, a simulation for chemical quantum computation using FEM is documented in [12] where we have used nanotubes immersed in polymer matrices.

We consider in this work a higher order FEM formulation to treat the elasticity problem. That is, the polynomial degree, which is arbitrary but fixed, is uniformly constant in the entire FEM mesh. We examine the a-posteriori error estimator locally within each element and each edge. There are several types of edges: the interface edges, the

interior edges, the exterior edges and the boundary edges. The error estimator can be efficiently computed element by element. In addition to the theoretical investigation, we contribute about the numerical influence of the parameters appearing in the a-posteriori error estimator. We need numerical tests because the dependence of all various constants with respect to the problem parameters is not established theoretically. The organization of this paper is structured as follows. In the next section, we describe the setting of the elastostatic problem together with the discretization utilizing higher order FEM. Afterwards, section 3 will be entirely occupied by the study of the polynomial inverse estimates. The theory for the a-posteriori estimates is elaborated in section 4. Some outcomes of numerical experiments are reported in the final section.

2. Problem setting and discretizations

We designate by $\mathbf{\Omega}$ an elastic model enclosed within $\mathbf{\Gamma} = \partial\mathbf{\Omega}$. It admits the elastic properties which are specified by the Lamé coefficients (λ, μ) whose relation with the Young's modulus E and the Poisson ratio ν is:

$$\lambda = \frac{E\nu}{(1+\nu)(1-2\nu)}, \qquad \mu = \frac{E}{2(1+\nu)}. \tag{2.2}$$

Since the coefficients (E, ν) and (λ, μ) are easily interchangeable, we adopt (λ, μ) from here onward. Throughout, vector values are supposed to be column vectors. Thus, the scalar product of $\mathbf{a}$ and $\mathbf{b}$ is denoted by $\mathbf{a}^{\mathrm{T}}\mathbf{b}$ while the norm is denoted by $|\mathbf{a}| = \sqrt{\mathbf{a}^{\mathrm{T}}\mathbf{a}}$. When the model $\mathbf{\Omega}$ is subject to a body force and prescribed boundary conditions, it has the displacement function

$$\mathbf{U} : \mathbf{\Omega} \longrightarrow \mathbb{R}^2 \qquad \text{where} \qquad \mathbf{U} = (U_1, U_2)^{\mathrm{T}}. \tag{2.3}$$

The strain tensor is defined as

$$\varepsilon_{ij}(\mathbf{U}(\mathbf{x})) := \frac{1}{2}\big(\partial_j U_i(\mathbf{x}) + \partial_i U_j(\mathbf{x})\big) \quad \text{for} \quad \mathbf{x} \in \mathbf{\Omega}. \tag{2.4}$$

According to the Hook's law for the stress-strain relation, the stress tensor is given by

$$\sigma_{ij}(\mathbf{U}) = \mu(\partial_j U_i + \partial_i U_j) + \lambda \sum_k (\partial_k U_k)\delta_{i,j} \tag{2.5}$$

$$= 2\mu\varepsilon_{ij}(\mathbf{U}) + \lambda(\operatorname{div}\mathbf{U})\delta_{i,j}. \tag{2.6}$$

In term of tensors where $\nabla\mathbf{U}$ denotes the matrix having $\partial_i U_j$ as coefficients, we have

$$\boldsymbol{\varepsilon}(\mathbf{U}) = \big[\varepsilon_{ij}(\mathbf{U})\big]_{i,j} = 0.5\big[(\nabla\mathbf{U}) + (\nabla\mathbf{U})^{\mathrm{T}}\big] \qquad \text{and} \qquad \boldsymbol{\sigma}(\mathbf{U}) = \big[\sigma_{ij}(\mathbf{U})\big]_{i,j}, \tag{2.7}$$

$$\begin{bmatrix} \sigma_{11}(\mathbf{U}) \\ \sigma_{22}(\mathbf{U}) \\ \sigma_{12}(\mathbf{U}) \end{bmatrix} = \begin{bmatrix} \lambda+2\mu & \lambda & 0 \\ \lambda & \lambda+2\mu & 0 \\ 0 & 0 & 2\mu \end{bmatrix} \begin{bmatrix} \varepsilon_{11}(\mathbf{U}) \\ \varepsilon_{22}(\mathbf{U}) \\ \varepsilon_{12}(\mathbf{U}) \end{bmatrix}. \tag{2.8}$$

We consider the interior Navier-Lamé equation with homogeneous Dirichlet boundary condition:

$$\left\{\begin{array}{lcll} -\mathrm{div}\big[\boldsymbol{\sigma}\big(\mathbf{U}(\mathbf{x})\big)\big] &=& \mathbf{f}(\mathbf{x}) & \text{for} \quad \mathbf{x}\in\boldsymbol{\Omega} \\ \boldsymbol{\sigma}\big(\mathbf{U}(\mathbf{x})\big) &=& 2\mu\boldsymbol{\varepsilon}\big(\mathbf{U}(\mathbf{x})\big)+\lambda\,\mathrm{Trace}\big[\boldsymbol{\varepsilon}\big(\mathbf{U}(\mathbf{x})\big)\big]\mathbf{I}_2 & \text{for} \quad \mathbf{x}\in\boldsymbol{\Omega} \\ \mathbf{U}(\mathbf{x}) &=& \mathbf{0} & \text{for} \quad \mathbf{x}\in\boldsymbol{\Gamma}=\partial\boldsymbol{\Omega} \end{array}\right. \tag{2.9}$$

in which $\mathbf{f}=[f_1,f_2]^{\mathrm{T}}$ represents a given body/volume force function. The space of square integrable scalar valued functions is

$$\mathbb{L}^2(\boldsymbol{\Omega}):=\Big\{f:\boldsymbol{\Omega}\to\mathbb{R},\qquad \int_{\boldsymbol{\Omega}}\big|f(\mathbf{x})\big|^2d\mathbf{x}<\infty\Big\}. \tag{2.10}$$

The Sobolev space on $\boldsymbol{\Omega}$ for a non-negative integer k is

$$\mathbb{H}^k(\boldsymbol{\Omega}):=\Big\{f\in\mathbb{L}^2(\boldsymbol{\Omega}):\ \big\|\partial^{\boldsymbol{\alpha}}f\big\|_{\mathbb{L}^2(\boldsymbol{\Omega})}<\infty\quad\text{for all}\quad|\boldsymbol{\alpha}|\le k\Big\} \tag{2.11}$$

where the differentiation $\partial^{\boldsymbol{\alpha}}f$ is interpreted in the sense of distribution such that $\langle\partial^{\boldsymbol{\alpha}}f,g\rangle_{\mathbb{L}^2(\boldsymbol{\Omega})}=(-1)^{|\boldsymbol{\alpha}|}\langle f,\partial^{\boldsymbol{\alpha}}g\rangle_{\mathbb{L}^2(\boldsymbol{\Omega})}$ for all compactly supported smooth functions g. The Sobolev space $\mathbb{H}^k(\boldsymbol{\Omega})$ is endowed with the norm

$$\big\|f\big\|^2_{\mathbb{H}^k(\boldsymbol{\Omega})}:=\sum_{|\boldsymbol{\alpha}|\le k}\big\|\partial^{\boldsymbol{\alpha}}f\big\|^2_{\mathbb{L}^2(\boldsymbol{\Omega})}. \tag{2.12}$$

The vector/matrix valued Sobolev spaces are componentwise of the scalar valued Sobolev spaces. The above Navier-Lamé equation corresponds to the partial differential operator $-\mu\Delta\mathbf{U}-(\mu+\lambda)\mathbf{grad}\,(\mathrm{div}\,\mathbf{U})$ which is associated to the bilinear form

$$\mathcal{A}(\mathbf{U},\mathbf{V}) := \int_{\boldsymbol{\Omega}}\sum_{i,j}2\mu\varepsilon_{ij}\big(\mathbf{U}(\mathbf{x})\big)\varepsilon_{ij}\big(\mathbf{V}(\mathbf{x})\big)+\lambda\mathrm{div}\big(\mathbf{U}(\mathbf{x})\big)\mathrm{div}\big(\mathbf{V}(\mathbf{x})\big)d\mathbf{x} \tag{2.13}$$

$$= \int_{\boldsymbol{\Omega}}\boldsymbol{\varepsilon}(\mathbf{U}(\mathbf{x})):\boldsymbol{\sigma}(\mathbf{V}(\mathbf{x}))\,d\mathbf{x} \tag{2.14}$$

where $A:B:=\sum_{i,j}A_{ij}B_{ij}$. The resulting energy norm $|\!|\!|\bullet|\!|\!|_E:=\mathcal{A}(\bullet,\bullet)^{1/2}$ is

$$\big|\!\big|\!\big|\mathbf{U}\big|\!\big|\!\big|^2_E=2\mu\big\|\boldsymbol{\varepsilon}(\mathbf{U})\big\|^2_{[L_2(\boldsymbol{\Omega})]^{2\times2}}+\lambda\big\|\mathrm{div}(\mathbf{U})\big\|^2_{[L_2(\boldsymbol{\Omega})]^2}. \tag{2.15}$$

One has the equivalence of the energy norm and the usual Sobolev norm:

$$C_1\|\mathbf{U}\|_{[\mathbb{H}^1(\boldsymbol{\Omega})]^2}\le|\!|\!|\mathbf{U}|\!|\!|_E\le C_2\|\mathbf{U}\|_{[\mathbb{H}^1(\boldsymbol{\Omega})]^2} \tag{2.16}$$

where C_1 does not depend on the elastic parameters due to the Korn's inequality while C_2 does. The conormal derivative of a function $\mathbf{u}$ is given componentwise by

$$[\boldsymbol{\gamma}_1\mathbf{u}]_i(\mathbf{x})=\sum_{j=1}^{2}\nu_j(\mathbf{x})\sigma_{ij}\big[\mathbf{u}(\mathbf{x})\big]. \tag{2.17}$$

In practical applications, the conormal derivative coincides with the traction. The Galerkin variational formulation is

$$\int_{\mathbf{\Omega}} \boldsymbol{\varepsilon}[\mathbf{U}(\mathbf{x})] : \boldsymbol{\sigma}[\mathbf{V}(\mathbf{x})] d\mathbf{x} = \int_{\mathbf{\Omega}} [\mathbf{f}(\mathbf{x})]^{\mathrm{T}} \mathbf{V}(\mathbf{x}) d\mathbf{x} \qquad \forall\, \mathbf{V} \in \left[\mathbb{H}_0^1(\mathbf{\Omega})\right]^2. \tag{2.18}$$

For the FEM treatment of the above problem, we use a mesh $\mathbb{M}_h(\mathbf{\Omega})$ composed of triangles admitting the next properties:

- The intersection of two different elements $T_i, T_j \in \mathbb{M}_h(\mathbf{\Omega})$ is either empty or a common node or a complete edge,
- We have the coverings:

$$\mathbf{\Omega} = \bigcup_{T \in \mathbb{M}_h(\mathbf{\Omega})} T.$$

For a triangle $T \in \mathbb{M}_h(\mathbf{\Omega})$, we denote

$$\begin{aligned}
h(T) &:= \text{diameter}(T) = \sup\left\{|\mathbf{x}-\mathbf{y}|,\, \mathbf{x},\mathbf{y} \in T\right\},\\
\rho(T) &:= \text{supremum of the diameters of all balls contained in } T,\\
\sigma(T) &:= h(T)/\rho(T) = \text{aspect ratio of } T,\\
\mathcal{N}_0(T) &:= \text{set of elements of } \mathbb{M}_h(\mathbf{\Omega}) \text{ sharing a vertex with } T,\\
\mathcal{N}_i(T) &:= \text{set of elements of } \mathbb{M}_h(\mathbf{\Omega}) \text{ sharing a vertex with } T' \in \mathcal{N}_{i-1}(T).
\end{aligned}$$

We use $\mathcal{N}(T)$ to denote $\mathcal{N}_i(T)$ for sufficiently large i. We assume quasi-uniformity in the sense that there exists a constant $\rho_0 > 0$ such that

$$\rho(T) \le \rho_0 < \infty \qquad \text{for all} \qquad T \in \mathbb{M}_h(\mathbf{\Omega}). \tag{2.19}$$

We define the following mutually disjoint subsets of edges

$$\begin{aligned}
\mathbb{E}_h^{\mathbf{0}} &:= \text{set of edges of } \mathbb{M}_h(\mathbf{\Omega}) \text{ on the boundary } \partial\mathbf{\Omega},\\
\mathbb{E}_h^{\mathbf{int}} &:= \text{set of edges of } \mathbb{M}_h(\mathbf{\Omega}) \text{ which are not included in } \mathbf{\Gamma}.
\end{aligned}$$

Note that an edge of $\mathbb{E}_h^{\mathbf{int}}$ may have an endpoint in $\mathbf{\Gamma}$. We introduce in addition the set of all edges

$$\mathbb{E}_h := \mathbb{E}_h^{\mathbf{0}} \cup \mathbb{E}_h^{\mathbf{int}}. \tag{2.20}$$

For an edge $e \in \mathbb{E}_h$, we denote

$$\begin{aligned}
h(e) &:= \text{length}(e) = \sup\left\{|\mathbf{x}-\mathbf{y}|,\, \mathbf{x},\mathbf{y} \in e\right\},\\
\mathcal{N}(e) &:= \text{set of elements of } \mathbb{M}_h \text{ having } e \text{ as a side},\\
\mathbf{n}(e) &:= \text{unit normal vector orthogonal to } e.
\end{aligned}$$

The direction of the normal vector $\mathbf{n}(e)$ is outward $\mathbf{\Gamma}$ for an edge $e \in \mathbb{E}_h^{\mathbf{0}}$ whereas it has an arbitrary but fixed orientation for an edge $e \in \mathbb{E}_h^{\mathbf{int}}$. For any triangle T, the affine invertible mapping from the unit reference

$$\widehat{T} := \Big\{ \mathbf{x} = (x, y) \in \mathbf{R}^2 : 0 \leq x \leq 1,\ 0 \leq y \leq 1,\ 0 \leq x + y \leq 1 \Big\} \tag{2.21}$$

onto T is denoted by $F_T : \widehat{T} :\longrightarrow T$ in which

$$F_T \mathbf{x} = B\mathbf{x} + b \quad \text{where} \quad \det(B) = \mathcal{O}(h^2(T)), \quad \det(B^{-1}) = \mathcal{O}(h^{-2}(T)). \tag{2.22}$$

From here onward, we use the usual shorthand $X \precsim Y$ if there is a constant c such that $X \leq cY$ in which c is independent on h and p. In addition, $X \simeq Y$ amounts to $X \precsim Y \precsim X$. For the higher order FEM setting, the finite dimensional subspace of $\big[\mathbb{H}_0^1(\mathbf{\Omega})\big]^2$ is

$$\mathcal{S}_h := \left\{ \mathbf{W} \in \Big[\mathcal{C}^0(\mathbf{\Omega}) \cap \mathbb{H}_0^1(\mathbf{\Omega})\Big]^2 \;\middle|\; \begin{array}{l} \mathbf{W} = (W_1, W_2), \\ W_i \in \mathcal{P}_p(T) \quad \forall\, T \in \mathbb{M}_h(\mathbf{\Omega}),\, \forall\, i = 1, 2 \end{array} \right\} \tag{2.23}$$

where $\mathcal{P}_p(T)$ denotes the space of polynomials in T spanned by the monomials $x^i y^j$ in which $0 \leq i + j \leq p$. The approximated variational formulation consists in searching for $\mathbf{U}_h \in \mathcal{S}_h$ such that

$$\int_{\mathbf{\Omega}} \boldsymbol{\varepsilon}\big[\mathbf{U}_h(\mathbf{x})\big] : \boldsymbol{\sigma}\big[\mathbf{V}_h(\mathbf{x})\big] d\mathbf{x} = \int_{\mathbf{\Omega}} \big[\mathbf{f}(\mathbf{x})\big]^{\mathrm{T}} \mathbf{V}_h(\mathbf{x}) d\mathbf{x} \qquad \forall\, \mathbf{V}_h \in \mathcal{S}_h. \tag{2.24}$$

3. Polynomial inverse estimates

In this section, we consider polynomial inverse estimates with respect to weighted Sobolev norms where some weight functions involving barycentric coordinates are utilized. For a triangle $T = \{(x_0, y_0), (x_1, y_1), (x_2, y_2)\}$, we recall the barycentric coordinates for $i = 0, 1, 2$ as the polynomial of degree unity

$$\lambda_{i,T}(x, y) := \frac{\begin{vmatrix} x - x_{i+1} & x_{i+2} - x_{i+1} \\ y - y_{i+1} & y_{i+2} - y_{i+1} \end{vmatrix}}{\begin{vmatrix} x_i - x_{i+1} & x_{i+2} - x_{i+1} \\ y_i - y_{i+1} & y_{i+2} - y_{i+1} \end{vmatrix}} \qquad \text{where} \qquad (x_3, y_3) \equiv (x_0, y_0). \tag{3.25}$$

For a triangle T, the barycentric weight function is expressed for $\mathbf{x} \in T$ as

$$\omega_T(\mathbf{x}) = \lambda_{0,T}(\mathbf{x}) \lambda_{1,T}(\mathbf{x}) \lambda_{2,T}(\mathbf{x}) \tag{3.26}$$

which takes zero values at the boundary of the triangle T. It is a generalization of the unidimensional Gegenbauer weight (also known as Jacobi weight) which is defined on the unit interval $[0, 1]$ as

$$\omega_{[0,1]}(t) := t(1 - t) \qquad \forall\, t \in [0, 1]. \tag{3.27}$$

The inverse estimate for the p-version is much more involved than that of the h-version. In the latter, one simply transforms the function onto the reference element. By using a simple norm equivalence on finite dimensional linear spaces, one deduces the results on the reference element which is transformed back to the original element.

LEMMA. *Given α, β such that $-1 < \alpha < \beta$ and some $\delta \in [0,1]$. For every univariate polynomial π_p of degree $p \geq 1$ on the 1D reference element $[0,1]$, one has*

$$\int_0^1 \big[\pi_p(t)\big]^2 \omega^{\alpha}_{[0,1]}(t)dt \;\leq\; C_1 p^{2(\beta-\alpha)} \int_0^1 \big[\pi_p(t)\big]^2 \omega^{\beta}_{[0,1]}(t)dt \tag{3.28}$$

$$\int_0^1 \big[\pi'_p(t)\big]^2 \omega^{2\delta}_{[0,1]}(t)dt \;\leq\; C_2 p^{2(2-\delta)} \int_0^1 \big[\pi_p(t)\big]^2 \omega^{\delta}_{[0,1]}(t)dt \tag{3.29}$$

$$\int_0^1 \big[\pi'_p(t)\big]^2 \omega_{[0,1]}(t)dt \;\leq\; C_3 p^2 \int_0^1 \big[\pi_p(t)\big]^2 \omega_{[0,1]}(t)dt. \tag{3.30}$$

The constants are $C_1 = C_1(\alpha,\beta)$, $C_2 = C_2(\delta)$, $C_3 = C_3(\alpha,\beta)$ which do not depend on p.

REMARK. Though in 1D, the above weighted polynomial inverse estimates on the unit interval is very complicated. It involves the expansion of a polynomial in Jacobi basis for which one uses the eigenvalues of the Jacobi polynomials. The representation of the integrals in the Sobolev norms is expressed in term of the Gauss-Lobatto quadrature points which admit good properties with respect to the Jacobi polynomials. We refer the interested readers to [19, 20, 37, 17, 9, 8] for more comprehensive analyses.

The following theorem has been documented in [19, 20] for the weight function

$$\omega_{\widehat{T}}(\mathbf{x}) = \text{distance}(\mathbf{x}, \partial\widehat{T}) \qquad \forall\, \mathbf{x} \in \widehat{T} \tag{3.31}$$

which is a bubble function vanishing at the boundary $\partial\widehat{T}$. We use instead the Gegenbauer weight whose advantage over (3.31) is that it is not expensive to evaluate in practical computations. In a-posteriori error estimation, the weights need to be explicitly evaluated and the next theorem is therefore not only important for theoretical reasons. Moreover, it is conceivable to evaluate some involved integrals analytically instead of using quadrature rules. In addition, the following estimates are interesting by themselves.

THEOREM. *Given α, β such that $-1 < \alpha < \beta$ and some $\delta \in [0,1]$. By using the generalized Gegenbauer weight*

$$\omega_{\widehat{T}}(\mathbf{x}) = \lambda_{0,\widehat{T}}(\mathbf{x})\lambda_{1,\widehat{T}}(\mathbf{x})\lambda_{2,\widehat{T}}(\mathbf{x}) = (1 - x_1 - x_2)x_1x_2 \tag{3.32}$$

for $\mathbf{x} = (x_1, x_2)$ on the 2D reference element

$$\widehat{T} = \Big\{\mathbf{x} = (x_1, x_2) \in \mathbf{R}^2 : 0 \leq x_1 \leq 1,\ 0 \leq x_2 \leq 1,\ 0 \leq x_1 + x_2 \leq 1\Big\}, \tag{3.33}$$

one has for every bivariate polynomial π_p of degree $p \geq 1$

$$\int_{\widehat{T}} \big[\pi_p(\mathbf{x})\big]^2 \omega_{\widehat{T}}^{\alpha}(\mathbf{x})d\mathbf{x} \leq C_1 p^{2(\beta-\alpha)} \int_{\widehat{T}} \big[\pi_p(\mathbf{x})\big]^2 \omega_{\widehat{T}}^{\beta}(\mathbf{x})d\mathbf{x} \tag{3.34}$$

$$\int_{\widehat{T}} \big|\nabla\pi_p(\mathbf{x})\big|^2 \omega_{\widehat{T}}^{2\delta}(\mathbf{x})d\mathbf{x} \leq C_2 p^{2(2-\delta)} \int_{\widehat{T}} \big[\pi_p(\mathbf{x})\big]^2 \omega_{\widehat{T}}^{\delta}(\mathbf{x})d\mathbf{x} \tag{3.35}$$

$$\int_{\widehat{T}} \big|\nabla\pi_p(\mathbf{x})\big|^2 \omega_{\widehat{T}}(\mathbf{x})d\mathbf{x} \leq C_3 p^2 \int_{\widehat{T}} \big[\pi_p(\mathbf{x})\big]^2 \omega_{\widehat{T}}(\mathbf{x})d\mathbf{x}. \tag{3.36}$$

The constants are $C_1 = C_1(\alpha,\beta)$, $C_2 = C_2(\delta)$, $C_3 = C_3(\alpha,\beta)$ which do not depend on p.

PROOF. To show (3.34), we proceed in several steps. Refer to Fig. 1(a) for the illustration of the involved notations. We subdivide the triangle $\widehat{T}$ into several overlapping subregions. We fix some constants $\boldsymbol{\theta} = (\theta_1,\theta_2)$, $\boldsymbol{\rho} = (\rho_1,\rho_2)$, $\mathbf{a}^0 = (a_0,b_0)$, $\mathbf{a}^1 = (a_1,b_1)$, $\mathbf{a}^2 = (a_2,b_2)$ and define

$$\mathbf{V}(\boldsymbol{\theta}) := \big\{\mathbf{x} = (x_1,x_2) \in \widehat{T} :\ \theta_1 \leq x_1 \leq \theta_2\big\} \tag{3.37}$$

$$\mathbf{U}(\boldsymbol{\rho}) := \big\{\mathbf{x} = (x_1,x_2) \in \widehat{T} :\ \rho_1 \leq x_2 \leq \rho_2\big\} \tag{3.38}$$

$$\mathbf{R}^0(\mathbf{a}^0) := \big\{\mathbf{x} = (x_1,x_2) \in \widehat{T} :\ 0 \leq x_1 \leq a_0,\ 0 \leq x_2 \leq b_0\big\} \tag{3.39}$$

$$\mathbf{R}^1(\mathbf{a}^1) := \big\{\mathbf{x} = (x_1,x_2) \in \widehat{T} :\ 0 \leq 1-x_1-x_2 \leq a_1,\ 0 \leq x_2 \leq b_1\big\} \tag{3.40}$$

$$\mathbf{R}^2(\mathbf{a}^2) := \big\{\mathbf{x} = (x_1,x_2) \in \widehat{T} :\ 0 \leq x_1 \leq a_2,\ 0 \leq 1-x_1-x_2 \leq b_2\big\} \tag{3.41}$$

with the properties: $0 < \theta_1 < \theta_2 < 1$, $0 < \rho_1 < \rho_2 < 1$, $\theta_1 \leq a_0 < 1/2$, $\rho_1 \leq b_0 < 1/2$, $1-\theta_2 \leq a_1 < 1/2$, $\rho_1 \leq b_1 < 1/2$, $\theta_1 \leq a_2 < 1/2$ and $1-\rho_2 \leq b_2 < 1/2$. As a first step, we consider the integration on the subregion $\mathbf{V}(\boldsymbol{\theta})$

$$\big\|\pi_p \omega_{\widehat{T}}^{\alpha/2}\big\|^2_{\mathbf{V}(\boldsymbol{\theta})} = \int_{\theta_1}^{\theta_2} \int_0^{1-x_1} \pi_p^2(x_1,x_2)\omega_{\widehat{T}}^{\alpha}(x_1,x_2)dx_1dx_2. \tag{3.42}$$

The generalized Gegenbauer weight is factorized as

$$\omega_{\widehat{T}}(x_1,x_2) = (1-x_1)\Big[\frac{1}{(1-x_1)^2}x_2(1-x_1-x_2)\Big]\big[x_1(1-x_1)\big] \tag{3.43}$$

$$= (1-x_1)\,\omega_{[0,1-x_1]}(x_2)\,\omega_{[0,1]}(x_1) \tag{3.44}$$

where

$$\omega_{[a,b]}(t) := \frac{(t-a)(b-t)}{(b-a)^2} \qquad \text{for} \qquad t \in [a,b]. \tag{3.45}$$

$$\begin{aligned}\big\|\pi_p\,\omega_{\widehat{T}}^{\alpha/2}\big\|^2_{\mathbf{V}(\boldsymbol{\theta})} &= \int_{\theta_1}^{\theta_2} \Big\{ \int_0^{1-x_1} (1-x_1)^{\alpha}\omega^{\alpha}_{[0,1-x_1]}(x_2)\omega^{\alpha}_{[0,1]}(x_1)\pi_p^2(x_1,x_2)dx_2\Big\}dx_1 \\ &= \int_{\theta_1}^{\theta_2} (1-x_1)^{\alpha}\omega^{\alpha}_{[0,1]}(x_1)\Big\{ \int_0^{1-x_1} \omega^{\alpha}_{[0,1-x_1]}(x_2)\pi_p^2(x_1,x_2)dx_2\Big\}dx_1.\end{aligned}$$

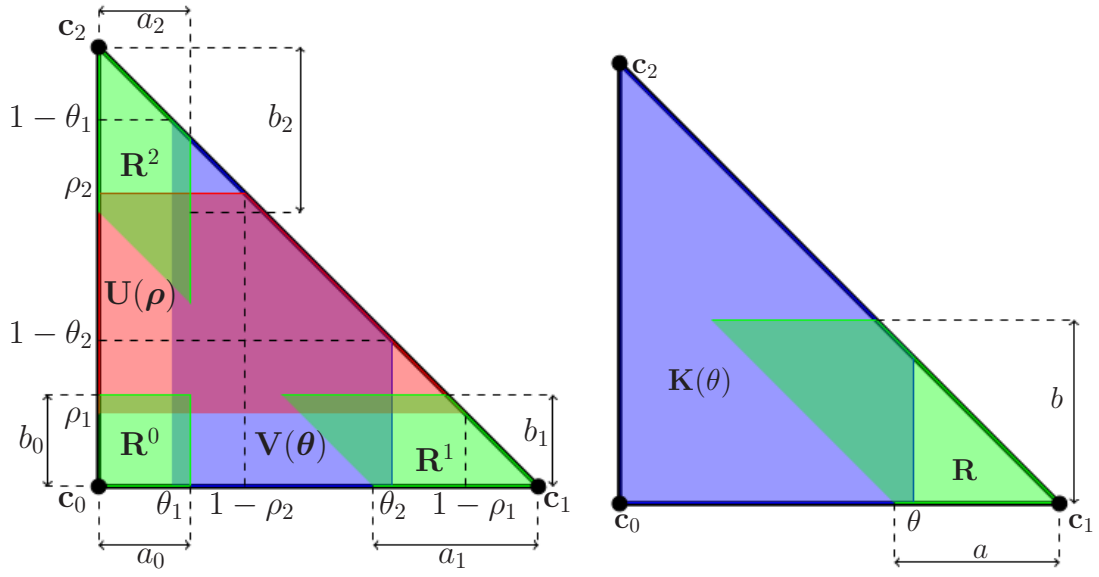

FIGURE 1. Illustration of the notations on the unit triangle $\widehat{T}$ where $\mathbf{c}_0=[0,0]$, $\mathbf{c}_1=[1,0]$, $\mathbf{c}_2=[0,1]$.

On the other hand, one has the following auxiliary univariate result for any $b\in]0,1[$ and for any univariate polynomial v_p by using the scaled 1D-weight (3.45) and the estimate (3.28)

$$\begin{aligned}\big\|v_p\,\omega_{[0,b]}^{\alpha/2}\big\|_{[0,b]}^2 &= \int_0^b \omega_{[0,1]}^{\alpha}(t)\big[v_p(t)\big]^2dt \le Cp^{2(\beta-\alpha)}b\int_0^1 \omega_{[0,1]}^{\beta}(t)\big[v_p(bt)\big]^2dt\\ &\le Cp^{2(\beta-\alpha)}\int_0^b \omega_{[0,b]}^{\beta}(t)\big[v_p(t)\big]^2dt = Cp^{2(\beta-\alpha)}\big\|v_p\,\omega_{[0,b]}^{\beta/2}\big\|_{[0,b]}^2\end{aligned}$$

where the constant C depends neither on p nor on b. Hence, for any fixed x_1, one has

$$\big\|\pi_p(x_1,\bullet)\omega_{[0,1-x_1]}^{\alpha/2}\big\|_{[0,1-x_1]}^2 \le Cp^{2(\beta-\alpha)}\big\|\pi_p(x_1,\bullet)\omega_{[0,1-x_1]}^{\beta/2}\big\|_{[0,1-x_1]}^2 \tag{3.46}$$

with C independent on x_1. As a consequence,

$$\begin{aligned}\|\pi_p\,\omega_{\widehat{T}}^{\alpha/2}\|_{\mathbf{V}(\boldsymbol{\theta})}^2 &\le Cp^{2(\beta-\alpha)}\int_{\theta_1}^{\theta_2}(1-x_1)^{\alpha}\omega_{[0,1]}^{\alpha}(x_1)\Big\{\int_0^{1-x_1}\omega_{[0,1-x_1]}^{\beta}(x_2)\pi_p^2\,dx_2\Big\}dx_1\\ &\precsim p^{2(\beta-\alpha)}\int_{\theta_1}^{\theta_2}\frac{1}{(1-x_1)^{(\beta-\alpha)}\omega_{[0,1]}^{\beta-\alpha}(x_1)}\times\\ &\qquad (1-x_1)^{\beta}\omega_{[0,1]}^{\beta}(x_1)\Big\{\int_0^{1-x_1}\omega_{[0,1-x_1]}^{\beta}(x_2)\pi_p^2\,dx_2\Big\}dx_1.\end{aligned}$$

The singularities of the function

$$t \longmapsto \frac{1}{(1-t)^{(\beta-\alpha)}\omega_{[0,1]}^{\beta-\alpha}(t)} \quad \text{are at } 0 \text{ and } 1 \tag{3.47}$$

which are not comprised in $[\theta_1, \theta_2]$ because $\alpha \leq \beta$. Consequently,

$$\sigma_1 \equiv \sigma_1(\alpha,\beta) := \sup_{t\in[\theta_1,\theta_2]} \frac{1}{(1-t)^{(\beta-\alpha)}\omega_{[0,1]}^{\beta-\alpha}(t)} < \infty. \tag{3.48}$$

Hence, by using (3.44) again, we deduce

$$\big\|\pi_p\,\omega_{\widehat{T}}^{\alpha/2}\big\|^2_{\mathbf{V}(\boldsymbol{\theta})} \precsim \sigma_1 p^{2(\beta-\alpha)} \int_{\theta_1}^{\theta_2} (1-x_1)^{\beta}\omega_{[0,1]}^{\beta}(x_1) \times \tag{3.49}$$

$$\Big\{ \int_0^{1-x_1} \omega_{[0,1-x_1]}^{\beta}(x_2)\pi_p^2\,dx_2\Big\}dx_1 \tag{3.50}$$

$$\precsim \sigma_1(\alpha,\beta)p^{2(\beta-\alpha)} \int_{\theta_1}^{\theta_2}\int_0^{1-x_1} \omega_{\widehat{T}}^{\beta}(x_1,x_2)\pi_p^2(x_1,x_2)\,dx_1dx_2 \tag{3.51}$$

$$\precsim \sigma_1(\alpha,\beta)p^{2(\beta-\alpha)}\big\|\pi_p\,\omega_{\widehat{T}}^{\beta/2}\big\|^2_{\mathbf{V}(\boldsymbol{\theta})}. \tag{3.52}$$

The next step is very similar to the former one except that we consider the subregion $\mathbf{U}(\boldsymbol{\rho})$ from (3.38) in order to obtain for some $\sigma_2 = \sigma_2(\alpha,\beta)$

$$\big\|\pi_p\,\omega_{\widehat{T}}^{\alpha/2}\big\|^2_{\mathbf{U}(\boldsymbol{\rho})} \precsim \sigma_2(\alpha,\beta)p^{2(\beta-\alpha)}\big\|\pi_p\,\omega_{\widehat{T}}^{\beta/2}\big\|^2_{\mathbf{U}(\boldsymbol{\rho})}. \tag{3.53}$$

Consider now the rectangular subregion $\mathbf{R}^0$. The barycentric component $\lambda_{0,\widehat{T}}(x_1,x_2) = 1-x_1-x_2$ is uniformly bounded because $\mathbf{R}^0$ does not touch the edge $[\mathbf{c}_1,\mathbf{c}_2]$:

$$0 < k_1 \leq \lambda_{0,\widehat{T}}(x_1,x_2) \leq k_2 < 1 \qquad \text{for} \qquad (x_1,x_2)\in\mathbf{R}^0 \tag{3.54}$$

where k_1 and k_2 are constants. Hence, we have the equivalence

$$\omega_{\widehat{T}}^{\alpha}(x_1,x_2) \simeq x_1^{\alpha}x_2^{\alpha} \qquad \text{for} \qquad (x_1,x_2)\in\mathbf{R}^0. \tag{3.55}$$

We consider first a polynomial in the form of a monomial $\pi(x_1,x_2) = \zeta_{i,j}x_1^i x_2^j$. We have

$$I_{i,j}(\alpha) := \int_{\mathbf{R}^0} \pi^2(x_1,x_2)x_1^{\alpha}x_2^{\alpha}\,dx_1dx_2 = \zeta_{i,j}^2\int_0^{a_0}\int_0^{b_0} x_1^{2i+\alpha}x_2^{2j+\alpha}dx_1dx_2 \tag{3.56}$$

$$= \zeta_{i,j}^2\Big(\frac{a_0^{2i+\alpha+1}}{2i+\alpha+1}\Big)\Big(\frac{b_0^{2j+\alpha+1}}{2j+\alpha+1}\Big). \tag{3.57}$$

Consider the quotient

$$\frac{I_{i,j}(\alpha)}{I_{i,j}(\beta)} = a_0^{\alpha-\beta}b_0^{\alpha-\beta}\Big(\frac{2i+\beta+1}{2i+\alpha+1}\Big)\Big(\frac{2j+\beta+1}{2j+\alpha+1}\Big) \tag{3.58}$$

$$= C(\alpha,\beta)\Big(\frac{2i+\beta+1}{2i+\alpha+1}\Big)\Big(\frac{2j+\beta+1}{2j+\alpha+1}\Big). \tag{3.59}$$

At limit, the factor

$$1 \leq \Big(\frac{2i+\beta+1}{2i+\alpha+1}\Big) \longrightarrow 1 \qquad \text{as} \qquad i \longrightarrow \infty. \tag{3.60}$$

For any $0 < \varepsilon < 1$, there is therefore $\eta \in \mathbb{N}$ sufficiently large such that

$$\frac{2i+\beta+1}{2i+\alpha+1} \leq 1+\varepsilon < 2 \qquad \text{for} \qquad i > \eta. \tag{3.61}$$

Define

$$\mu_0 := \max\Big\{\frac{2i+\beta+1}{2i+\alpha+1} : \, i = 0, \cdots, \eta\Big\}. \tag{3.62}$$

The same thing holds true for the second factor in (3.59). Hence, by using the fact that $p \geq 1$ and $\beta \geq \alpha$, we deduce

$$I_{i,j}(\alpha) \precsim \mu_0 C(\alpha,\beta) I_{i,j}(\beta) \precsim \sigma_3^0(\alpha,\beta) p^{2(\beta-\alpha)} I_{i,j}(\beta). \tag{3.63}$$

Decompose any general polynomial π_p in term of monomials and use the equivalence (3.55) to obtain

$$\big\|\pi_p\, \omega_{\widehat{T}}^{\alpha/2}\big\|_{\mathbf{R}^0}^2 \precsim \sigma_3^{(0)}(\alpha,\beta) p^{2(\beta-\alpha)} \big\|\pi_p\, \omega_{\widehat{T}}^{\beta/2}\big\|_{\mathbf{R}^0}^2. \tag{3.64}$$

We describe partially the case of the parallelogram $\mathbf{R}^1$. As in (3.55), since $\mathbf{R}^1$ does not touch the edge $[\mathbf{c}_0, \mathbf{c}_2]$, we obtain the equivalence

$$\omega_{\widehat{T}}^{\alpha}(x_1,x_2) \simeq x_2^{\alpha}(1-x_1-x_2)^{\alpha} \qquad \text{for} \qquad (x_1,x_2) \in \mathbf{R}^1. \tag{3.65}$$

We consider the invertible affine transform

$$\begin{bmatrix} x_1 \\ x_2 \end{bmatrix} = \begin{bmatrix} -1 & -1 \\ 0 & 1 \end{bmatrix} \begin{bmatrix} \widetilde{x}_1 \\ \widetilde{x}_2 \end{bmatrix} + \begin{bmatrix} 1 \\ 0 \end{bmatrix} \tag{3.66}$$

which is a bilinear transform from the rectangle

$$\widetilde{\mathbf{R}}^1 := \big\{(\widetilde{x}_1,\widetilde{x}_2) : \, 0 \leq \widetilde{x}_1 \leq a_1, \quad 0 \leq \widetilde{x}_2 \leq b_1\big\} \tag{3.67}$$

onto the parallelogram $\mathbf{R}^1$. We proceed as before on the rectangle $\widetilde{\mathbf{R}}^1$ by noting that $\omega_{\widehat{T}} \simeq \widetilde{x}_1^{\alpha}\widetilde{x}_2^{\alpha}$ for $(\widetilde{x}_1,\widetilde{x}_2) \in \widetilde{\mathbf{R}}^1$ where every polynomial is decomposed into monomials $\zeta_{i,j}\widetilde{x}_1^i\widetilde{x}_2^j$. The remainder of the deduction is as above and we have the estimate

$$\big\|\pi_p\, \omega_{\widehat{T}}^{\alpha/2}\big\|_{\mathbf{R}^1}^2 \precsim \sigma_3^{(1)}(\alpha,\beta) p^{2(\beta-\alpha)} \big\|\pi_p\, \omega_{\widehat{T}}^{\beta/2}\big\|_{\mathbf{R}^1}^2. \tag{3.68}$$

The case of the parallelogram $\mathbf{R}^2$ is treated in the same manner by using an appropriate transform to obtain

$$\big\|\pi_p\, \omega_{\widehat{T}}^{\alpha/2}\big\|_{\mathbf{R}^2}^2 \precsim \sigma_3^{(2)}(\alpha,\beta) p^{2(\beta-\alpha)} \big\|\pi_p\, \omega_{\widehat{T}}^{\beta/2}\big\|_{\mathbf{R}^2}^2. \tag{3.69}$$

Define $\mathbf{R} := \mathbf{R}^0 \cup \mathbf{R}^1 \cup \mathbf{R}^2$ to obtain from (3.64), (3.68) and (3.69)

$$\big\|\pi_p\, \omega_{\widehat{T}}^{\alpha/2}\big\|_{\mathbf{R}}^2 \precsim \sigma_3(\alpha,\beta) p^{2(\beta-\alpha)} \big\|\pi_p\, \omega_{\widehat{T}}^{\beta/2}\big\|_{\mathbf{R}}^2 \quad \text{where} \tag{3.70}$$

$$\sigma_3(\alpha,\beta) := \max\big\{\sigma_3^{(0)}(\alpha,\beta), \sigma_3^{(1)}(\alpha,\beta), \sigma_3^{(2)}(\alpha,\beta)\big\}. \tag{3.71}$$

The conditions following the definitions (3.37)–(3.41) on the parameters $\boldsymbol{\theta}$, $\boldsymbol{\rho}$, $\mathbf{a}^0$, $\mathbf{a}^1$, $\mathbf{a}^2$ ensure that the union of the subregions $\mathbf{V}(\boldsymbol{\theta})$, $\mathbf{U}(\boldsymbol{\rho})$ and $\mathbf{R}$ entirely covers the triangle $\widehat{T}$. Whence we deduce

$$\big\|\pi_p\,\omega_{\widehat{T}}^{\alpha/2}\big\|_{\widehat{T}}^2 \leq \big\|\pi_p\,\omega_{\widehat{T}}^{\alpha/2}\big\|_{\mathbf{V}(\boldsymbol{\theta})}^2 + \big\|\pi_p\,\omega_{\widehat{T}}^{\alpha/2}\big\|_{\mathbf{U}(\boldsymbol{\rho})}^2 + \big\|\pi_p\,\omega_{\widehat{T}}^{\alpha/2}\big\|_{\mathbf{R}}^2. \tag{3.72}$$

By applying (3.52), (3.53), (3.70) respectively on each of the above terms, we obtain

$$\begin{aligned}\big\|\pi_p\,\omega_{\widehat{T}}^{\alpha/2}\big\|_{\widehat{T}}^2 \;\precsim\; & p^{2(\beta-\alpha)}\Big\{\sigma_1(\alpha,\beta)\big\|\pi_p\,\omega_{\widehat{T}}^{\beta/2}\big\|_{\mathbf{V}(\boldsymbol{\theta})}^2 + \sigma_2(\alpha,\beta)\big\|\pi_p\,\omega_{\widehat{T}}^{\beta/2}\big\|_{\mathbf{U}(\boldsymbol{\rho})}^2 + \qquad (3.73)\\ & \sigma_3(\alpha,\beta)\big\|\pi_p\,\omega_{\widehat{T}}^{\beta/2}\big\|_{\mathbf{R}}^2\Big\}. \qquad (3.74)\end{aligned}$$

Since we deal with positive integrands and $\mathbf{V}(\boldsymbol{\theta}) \subset \widehat{T}$, $\mathbf{U}(\boldsymbol{\rho}) \subset \widehat{T}$, $\mathbf{R} \subset \widehat{T}$, we have

$$\max\Big\{\big\|\pi_p\,\omega_{\widehat{T}}^{\beta/2}\big\|_{\mathbf{V}(\boldsymbol{\theta})}^2,\, \big\|\pi_p\,\omega_{\widehat{T}}^{\beta/2}\big\|_{\mathbf{U}(\boldsymbol{\rho})}^2,\, \big\|\pi_p\,\omega_{\widehat{T}}^{\beta/2}\big\|_{\mathbf{R}}^2\Big\} \leq \big\|\pi_p\,\omega_{\widehat{T}}^{\beta/2}\big\|_{\widehat{T}}^2. \tag{3.75}$$

Take therefore $C_1(\alpha,\beta) := \max\big\{\sigma_1(\alpha,\beta), \sigma_2(\alpha,\beta), \sigma_3(\alpha,\beta)\big\}$ to deduce

$$\big\|\pi_p\,\omega_{\widehat{T}}^{\alpha/2}\big\|_{\widehat{T}}^2 \precsim C_1(\alpha,\beta)p^{2(\beta-\alpha)}\big\|\pi_p\,\omega_{\widehat{T}}^{\beta/2}\big\|_{\widehat{T}}^2 \tag{3.76}$$

and we eventually obtain (3.34). Concerning (3.35), we proceed as before but now the subregions are:

$$\mathbf{K}(\theta) \;:=\; \big\{\mathbf{x}=(x_1,x_2)\in\widehat{T}:\, 0\leq x_1\leq\theta\big\} \tag{3.77}$$

$$\mathbf{R}(\mathbf{a}) \;:=\; \big\{\mathbf{x}=(x_1,x_2)\in\widehat{T}:\, 0\leq 1-x_1-x_2\leq a,\, 0\leq x_2\leq b\big\} \tag{3.78}$$

where the parameters $\theta, \mathbf{a}=(a,b)$ are chosen so that the two domains overlap and that they entirely cover $\widehat{T}$ as in Fig. 1(b). We have the next auxiliary 1D-result for any $0<b<1$ and any univariate polynomial v_p from a transformation of (3.29):

$$\big\|\omega_{[0,b]}^{\delta}v_p'\big\|_{[0,b]}^2 \leq C\frac{1}{b^2}p^{2(2-\delta)}\big\|\omega_{[0,b]}^{\delta/2}v_p\big\|_{[0,b]}^2 \tag{3.79}$$

where the constant C is independent on p and b. By proceeding as before and by applying (3.79) to the polynomial $\partial_2\pi_p(x_1,\bullet)$, we obtain

$$\begin{aligned}\big\|\omega_{\widehat{T}}^{\delta}\partial_2\pi_p\big\|_{\mathbf{K}(\theta)}^2 \;=\; & \int_0^{\theta}\omega_{[0,1]}^{2\delta}(x_1)(1-x_1)^{2\delta}\Big\{\int_0^{1-x_1}\omega_{[0,1-x_1]}^{2\delta}(x_2)[\partial_2\pi_p]^2dx_2\Big\}dx_1\\ \precsim\; & \int_0^{\theta}\omega_{[0,1]}^{2\delta}(x_1)(1-x_1)^{2\delta}\Big\{\frac{1}{(1-x_1)^2}p^{2(2-\delta)}\int_0^{1-x_1}\omega_{[0,1-x_1]}^{\delta}(x_2)\pi_p^2dx_2\Big\}dx_1\\ \precsim\; & p^{2(2-\delta)}\int_0^{\theta}\Big(\omega_{[0,1]}^{\delta}(x_1)(1-x_1)^{\delta-2}\Big)\Big(\omega_{[0,1]}^{\delta}(x_1)(1-x_1)^{\delta}\Big)\times\\ & \Big\{\int_0^{1-x_1}\omega_{[0,1-x_1]}^{\delta}(x_2)\pi_p^2dx_2\Big\}dx_1.\end{aligned}$$

As done in (3.48), we have for $\delta\in[0,1]$

$$\sigma(\delta) := \sup_{x_1\in[0,\theta]}\omega_{[0,1]}^{\delta}(x_1)(1-x_1)^{\delta-2} = \sup_{x_1\in[0,\theta]}\frac{x_1^{\delta}}{(1-x_1)^{2(1-\delta)}} < \infty. \tag{3.80}$$

As a consequence, we deduce

$$\begin{aligned}\big\|\omega_{\widehat{T}}^{\delta}\partial_2\pi_p\big\|_{\mathbf{K}(\theta)}^2 &\precsim \sigma(\delta)p^{2(2-\delta)}\int_0^{\theta}\omega_{[0,1]}^{\delta}(x_1)(1-x_1)^{\delta}\Big\{\int_0^{1-x_1}\omega_{[0,1-x_1]}^{\delta}(x_2)\pi_p^2dx_2\Big\}dx_1\\ &\precsim \sigma(\delta)p^{2(2-\delta)}\big\|\omega_{\widehat{T}}^{\delta/2}\pi_p\big\|_{\mathbf{K}(\theta)}^2.\end{aligned}$$

Concerning the parallelogram $\mathbf{R}=\mathbf{R}(\mathbf{a})$, apply an affine transform as in (3.66) and obtain for a monomial $\pi=\zeta_{i,j}\widetilde{x}_1^i\widetilde{x}_2^j$

$$J_{i,j} := \big\|\omega_{\widehat{T}}^{\delta}\partial_2\pi\big\|_{\widetilde{\mathbf{R}}}^2=\zeta_{i,j}^2\int_{\widetilde{\mathbf{R}}}\widetilde{x}_1^{2\delta}\widetilde{x}_2^{2\delta}\widetilde{x}_1^{2i}j^2\widetilde{x}_2^{(2j-2)}d\widetilde{x}_1d\widetilde{x}_2 \tag{3.81}$$

$$= j^2\zeta_{i,j}^2\Big(\frac{a^{2\delta+2i+1}}{2\delta+2i+1}\Big)\Big(\frac{b^{2\delta+2j-1}}{2\delta+2j-1}\Big) \tag{3.82}$$

$$L_{i,j} := \big\|\omega_{\widehat{T}}^{\delta/2}\pi\big\|_{\widetilde{\mathbf{R}}}^2=\zeta_{i,j}^2\Big(\frac{a^{\delta+2i+1}}{\delta+2i+1}\Big)\Big(\frac{b^{\delta+2j-1}}{\delta+2j-1}\Big). \tag{3.83}$$

Hence, we have the next limit for the quotient

$$\frac{J_{i,j}}{L_{i,j}}=j^2\underbrace{a^{\delta}b^{\delta-2}}_{C(\delta)}\Big(\underbrace{\frac{\delta+2i+1}{2\delta+2i+1}}_{\longrightarrow 1}\Big)\Big(\underbrace{\frac{\delta+2j+1}{2\delta+2j-1}}_{\longrightarrow 1}\Big). \tag{3.84}$$

Proceed as before to deduce for any polynomial π_p

$$\Big\|\omega_{\widehat{T}}^{\delta}\frac{\partial\pi_p}{\partial\widetilde{x}_2}\Big\|_{\widetilde{\mathbf{R}}}^2\leq C(\delta)p^{2(2-\delta)}\big\|\omega_{\widehat{T}}^{\delta/2}\pi_p\big\|_{\widetilde{\mathbf{R}}}^2. \tag{3.85}$$

A similar procedure is applied to obtain a corresponding result for the partial derivative with respect to $\widetilde{x}_1$

$$\Big\|\omega_{\widehat{T}}^{\delta}\frac{\partial\pi_p}{\partial\widetilde{x}_1}\Big\|_{\widetilde{\mathbf{R}}}^2\leq C(\delta)p^{2(2-\delta)}\big\|\omega_{\widehat{T}}^{\delta/2}\pi_p\big\|_{\widetilde{\mathbf{R}}}^2. \tag{3.86}$$

Combine (3.85) and (3.86) and use the boundedness of the Jacobian of the affine transform in (3.66) to obtain on the parallelogram $\mathbf{R}$:

$$\Big\|\omega_{\widehat{T}}^{\delta}\frac{\partial\pi_p}{\partial x_2}\Big\|_{\mathbf{R}}^2\leq C(\delta)p^{2(2-\delta)}\big\|\omega_{\widehat{T}}^{\delta/2}\pi_p\big\|_{\mathbf{R}}^2. \tag{3.87}$$

Use the overlapping covering of $\widehat{T}$ by $\mathbf{K}(\theta)$ and $\mathbf{R}$ as done in (3.72) to obtain the result for $\partial/\partial x_2$ on the whole unit triangle. One repeats the same thing for $\partial/\partial x_1$ to obtain the result (3.35) with respect to the gradient $\nabla\pi_p$. We skip the deduction of the last estimate (3.36) which is treated very similarly as the preceding two estimates (3.34) and (3.35).

■

4. Elastostatic error estimator

Based on the former polynomial inverse estimates, we concentrate in this section on the investigation of the a-posteriori error estimator for the elastostatic problem by using higher order FEM. Thus, we suppose that we dispose of the approximated solution $\mathbf{U}_h$ and our purpose is to estimate the error $\|\mathbf{U}-\mathbf{U}_h\|_{[\mathbb{H}^1(\mathbf{\Omega})]^2}$. For an element $T\in\mathbb{M}_h(\mathbf{\Omega})$, the estimator is defined as

$$\eta^{\mathbf{tri}}_{\alpha,T}:=\frac{h(T)}{p}\Big\|\big(\mathbf{f}_T+\mu\Delta\mathbf{U}_h+(\mu+\lambda)\mathbf{grad}(\operatorname{div}\mathbf{U}_h)\big)\omega_T^{\alpha/2}\Big\|_{\left[\mathbb{L}^2(T)\right]^2} \tag{4.88}$$

where $\mathbf{f}_T$ designates the $\mathbb{L}_2(T)$-projection of the body force $\mathbf{f}$ onto the element T.

The estimator for an interior edge $e\in\mathbb{E}_h$ having a normal vector $\mathbf{n}(e)$ is defined by means of the stress tensor $\boldsymbol{\sigma}(\mathbf{U}_h)$ as

$$\eta^{\mathbf{edg}}_{\alpha,e}:=\sqrt{\frac{h(e)}{2p}}\Big\|\big(\boldsymbol{\sigma}(\mathbf{U}_h)_{|_{T_{(1,e)}}}\mathbf{n}(e)-\boldsymbol{\sigma}(\mathbf{U}_h)_{|_{T_{(2,e)}}}\mathbf{n}(e)\big)\omega_e^{\alpha/2}\Big\|_{\left[\mathbb{L}^2(e)\right]^2} \tag{4.89}$$

where $T_{(1,e)}$ and $T_{(2,e)}$ are the elements incident upon the edge e.

Since one needs computable local estimators for an element-by-element computation, an interior element $T\in\mathbb{M}_h(\mathbf{\Omega})$ is introduced

$$\eta^{\mathbf{loc}}_{\alpha,T}:=\Big[(\eta^{\mathbf{tri}}_{\alpha,T})^2+\sum_{e\subset\partial T,\,e\in\mathbb{E}_h^{\mathbf{int}}}(\eta^{\mathbf{edg}}_{\alpha,e})^2\Big]^{1/2} \tag{4.90}$$

The local estimators add up to the global estimator:

$$\eta_\alpha:=\sqrt{\sum_{T\in\mathbb{M}_h(\mathbf{\Omega})}(\eta^{\mathbf{loc}}_{\alpha,T})^2}. \tag{4.91}$$

The next lemma is developed in [19].

LEMMA. *Consider a univariate polynomial π of degree $p\geq 1$ defined on the unit reference interval $\widehat{e}=[0,1]$ and a parameter $0<\gamma\leq 1$. There exists a bivariate extension $v\in\mathbb{H}^1(\widehat{T})$ defined on the reference triangle $\widehat{T}$ from (2.21) such that it has the next properties w.r.t. the weight $\omega^\alpha_{\widehat{e}}$:*

$$v|_{\widehat{e}} \;=\; \pi\omega^\alpha_{\widehat{e}} \qquad \textit{and} \qquad v\big|_{(\partial\widehat{T}\setminus\widehat{e})}\equiv 0 \tag{4.92}$$

$$\|v\|^2_{\mathbb{L}_2(\widehat{T})} \;\leq\; C(\alpha)\gamma\|\pi\omega^{\alpha/2}_{\widehat{e}}\|^2_{\mathbb{L}_2(\widehat{e})} \tag{4.93}$$

$$\|\nabla v\|^2_{\mathbb{L}_2(\widehat{T})} \;\leq\; C(\alpha)\big[\gamma p^{2(2-\alpha)}+\gamma^{-1}\big]\|\pi\omega^{\alpha/2}_{\widehat{e}}\|^2_{\mathbb{L}_2(\widehat{e})}. \tag{4.94}$$

THEOREM. *For an element $T\in\mathbb{M}_h(\mathbf{\Omega})$, introduce the weighted oscillation*

$$\mathrm{OSC}(\mathbf{f},\mathbf{f}_T,\alpha,T):=\|(\mathbf{f}_T-\mathbf{f})\omega_T^{\alpha/2}\|_{[\mathbb{L}_2(T)]^2}. \tag{4.95}$$

One has as an upper bound of the bubble estimator $\eta_{\alpha,T}^{\mathbf{tri}}$ for a polynomial degree p:

$$\eta_{\alpha,T}^{\mathbf{tri}} \precsim C_p \|\mathbf{U}-\mathbf{U}_h\|_{[\mathbb{H}^1(T)]^2} + \frac{h(T)}{p}\mathrm{OSC}(\mathbf{f},\mathbf{f}_T,\alpha,T). \tag{4.96}$$

By using the oscillation

$$\mathrm{OSC}(\mathbf{f},\mathbf{f}_h,A) := \|\mathbf{f}-\mathbf{f}_h\|_{[\mathbb{L}^2(A)]^2}, \tag{4.97}$$

one has for the edge estimator $\eta_{\alpha,e}^{\mathbf{edg}}$ of an edge e

$$\eta_{\alpha,e}^{\mathbf{edg}} \precsim C_p \|\mathbf{U}-\mathbf{U}_h\|_{[\mathbb{H}^1(\mathcal{N}(e))]^2} + \frac{h(e)}{\sqrt{p}}\mathrm{OSC}(\mathbf{f},\mathbf{f}_h,\mathcal{N}(e)) \tag{4.98}$$

and in addition

$$\|\mathbf{U}-\mathbf{U}_h\|_{[\mathbb{H}^1(\mathbf{\Omega})]^2} \precsim C_p\eta_\alpha + \sum_{T\in\mathbb{M}_h(\mathbf{\Omega})}\frac{h(T)}{p}\mathrm{OSC}(\mathbf{f},\mathbf{f}_T,T). \tag{4.99}$$

PROOF.

Efficiency: Introduce

$$\mathbf{\Psi}_T := \Big[\mathbf{f}_T + \mu\Delta\mathbf{U}_h + (\lambda+\mu)\mathbf{grad}(\mathrm{div}(\mathbf{U}_h))\Big]\omega_T^\alpha. \tag{4.100}$$

We want first to estimate $|\mathbf{\Psi}_T|^2_{[\mathbb{H}^1(T)]^2}$ where

$$|\mathbf{\Psi}_T|^2_{[\mathbb{H}^1(T)]^2} = \sum_j |\nabla\Psi_{T,j}|_{[\mathbb{L}_2(T)]^2} \quad \text{in which} \quad \mathbf{\Psi}_T =: [\Psi_{T,1},\Psi_{T,2}]^{\mathrm{T}}. \tag{4.101}$$

In term of the componentwise stress tensor, we have

$$\Psi_{T,j} = \Big[f_{T,j} + \sum_{i=1}^{2}\partial_i[\sigma_{ij}(\mathbf{U}_h)]\Big]\omega_T^\alpha \tag{4.102}$$

$$\big|\nabla\Psi_{T,j}\big|^2_{[\mathbb{L}_2(T)]^2} \precsim \int_T \Big[f_{T,j} + \sum_i \partial_i[\sigma_{ij}(\mathbf{U}_h)]\Big]^2\big|\nabla\omega_T^\alpha\big|^2 + \tag{4.103}$$

$$\int_T \Big|\nabla\{f_{T,j} + \sum_i \partial_i[\sigma_{ij}(\mathbf{U}_h)]\}\Big|^2\omega_T^{2\alpha}. \tag{4.104}$$

In order to estimate the term in (4.103), we have for any $\widehat{\mathbf{x}} = (\widehat{x}_1,\widehat{x}_2) \in \widehat{T}$

$$\big[\partial_1\omega_{\widehat{T}}^\alpha(\widehat{\mathbf{x}})\big]^2 = \big[(-\alpha)(1-\widehat{x}_1-\widehat{x}_2)^{\alpha-1}\widehat{x}_1^\alpha\widehat{x}_2^\alpha + \alpha(1-\widehat{x}_1-\widehat{x}_2)^\alpha\widehat{x}_1^{\alpha-1}\widehat{x}_2^\alpha\big]^2 \tag{4.105}$$

$$\simeq (1-\widehat{x}_1-\widehat{x}_2)^{2(\alpha-1)}\widehat{x}_1^{2\alpha}\widehat{x}_2^{2\alpha} + (1-\widehat{x}_1-\widehat{x}_2)^{2\alpha}\widehat{x}_1^{2(\alpha-1)}\widehat{x}_2^{2\alpha} \tag{4.106}$$

$$\simeq \omega_{\widehat{T}}^{2(\alpha-1)}(\widehat{\mathbf{x}})\big[\widehat{x}_1^2\widehat{x}_2^2 + (1-\widehat{x}_1-\widehat{x}_2)^2\widehat{x}_2^2\big] \le 2\omega_{\widehat{T}}^{2(\alpha-1)}(\widehat{\mathbf{x}}). \tag{4.107}$$

By using a similar estimate for $\partial_2\omega_{\widehat{T}}^\alpha(\widehat{\mathbf{x}})$, obtain

$$\big|\nabla_{\widehat{\mathbf{x}}}\,\omega_{\widehat{T}}^\alpha(\widehat{\mathbf{x}})\big|^2 \precsim \omega_{\widehat{T}}^{2(\alpha-1)}(\widehat{\mathbf{x}}) \qquad \text{for all} \quad \widehat{\mathbf{x}}\in\widehat{T}. \tag{4.108}$$

With the help of the affine transform $F_T : \widehat{T} \longrightarrow T$ and the barycentric coordinates $\lambda_{i,T}(\mathbf{x}) = \lambda_{i,\widehat{T}}(F_T^{-1}(\mathbf{x}))$ for $\mathbf{x} = F_T(\widehat{\mathbf{x}}) \in T$, obtain

$$\left|\nabla_{\mathbf{x}}\,\omega_T^{\alpha}(\mathbf{x})\right|^2 = \left|(\mathbf{D}F_T^{-1})\nabla_{\widehat{\mathbf{x}}}\,\omega_{\widehat{T}}^{\alpha}(\widehat{\mathbf{x}})\right|^2 \precsim \frac{1}{h^2(T)}\left|\nabla_{\widehat{\mathbf{x}}}\,\omega_{\widehat{T}}^{\alpha}(\widehat{\mathbf{x}})\right|^2 \tag{4.109}$$

$$\precsim \frac{1}{h^2(T)}\omega_{\widehat{T}}^{2(\alpha-1)}(\widehat{\mathbf{x}}) = \frac{1}{h^2(T)}\omega_T^{2(\alpha-1)}(\mathbf{x}). \tag{4.110}$$

Hence, for each $j = 1, 2$, we deduce for the stress tensor σ_{ij}

$$\int_T \Big[f_{T,j}+\sum_i \partial_i[\sigma_{ij}(\mathbf{U}_h)]\Big]^2\left|\nabla\omega_T^{\alpha}\right|^2 \precsim \frac{1}{h^2(T)}\int_T \Big[f_{T,j}+\sum_i \partial_i[\sigma_{ij}(\mathbf{U}_h)]\Big]^2\omega_T^{2(\alpha-1)}. \tag{4.111}$$

Apply the polynomial inverse estimate (3.34) and the determinant properties (2.22) to the polynomial $\pi_p := f_{T,j} + \sum_i \partial_i[\sigma_{ij}(\mathbf{U}_h)]$

$$\left\|\pi_p\omega_T^{(\alpha-1)}\right\|^2_{\mathbb{L}_2(T)} = \int_{\widehat{T}} \widehat{\pi}_p^2(\widehat{\mathbf{x}})\,\omega_{\widehat{T}}^{2(\alpha-1)}(\widehat{\mathbf{x}})\det\left|\mathbf{D}F_T(\widehat{\mathbf{x}})\right|d\widehat{\mathbf{x}} \tag{4.112}$$

$$\precsim h^2(T)p^{2(2-\alpha)}\left\|\widehat{\pi}_p\omega_{\widehat{T}}^{\alpha/2}\right\|^2_{\mathbb{L}_2(\widehat{T})} \tag{4.113}$$

$$= h^2(T)p^{2(2-\alpha)}\int_T \pi_p^2(\mathbf{x})\omega_T^{\alpha}(\mathbf{x})\det\left|\mathbf{D}F_T^{-1}(\mathbf{x})\right|d\mathbf{x} \tag{4.114}$$

$$\precsim p^{2(2-\alpha)}\left\|\pi_p\omega_T^{\alpha/2}\right\|^2_{\mathbb{L}_2(T)}. \tag{4.115}$$

A combination of the last inequality and (4.111) reveals

$$\int_T \Big[f_{T,j}+\sum_i \partial_i[\sigma_{ij}(\mathbf{U}_h)]\Big]^2\left|\nabla\omega_T^{\alpha}\right|^2 \precsim \frac{p^{2(2-\alpha)}}{h^2(T)}\int_T \Big[f_{T,j}+\sum_i \partial_i[\sigma_{ij}(\mathbf{U}_h)]\Big]^2\omega_T^{\alpha}. \tag{4.116}$$

Concerning the term in (4.104), proceed similarly but with respect to the polynomial inverse estimate (3.35) where $\delta \equiv \alpha$ and obtain

$$\int_T \Big|\nabla\{f_{T,j}+\sum_i \partial_i[\sigma_{ij}(\mathbf{U}_h)]\}\Big|^2\omega_T^{2\alpha} \precsim \frac{p^{2(2-\alpha)}}{h^2(T)}\int_T \Big[f_{T,j}+\sum_i \partial_i[\sigma_{ij}(\mathbf{U}_h)]\Big]^2\omega_T^{\alpha}. \tag{4.117}$$

By combining the last two estimates for $j = 1, 2$, obtain

$$|\mathbf{\Psi}_T|^2_{[\mathbb{H}^1(T)]^2} \precsim \frac{p^{2(2-\alpha)}}{h^2(T)}\int_T \sum_{j=1}^{2}\Big[f_{T,j}+\sum_i \partial_i[\sigma_{ij}(\mathbf{U}_h)]\Big]^2\omega_T^{\alpha} \tag{4.118}$$

$$= \frac{p^{2(2-\alpha)}}{h^2(T)}\|\mathbf{\Psi}_T\omega^{-\alpha/2}\|^2_{[\mathbb{L}_2(T)]^2}. \tag{4.119}$$

On the other hand, according to the definition of $\mathbf{\Psi}_T$ and by using (4.119), obtain

$$\begin{aligned}
\|\mathbf{\Psi}_T\omega^{-\alpha/2}\|^2_{[\mathbb{L}_2(T)]^2} &= \int_T \big|\mathbf{f}_T+\mu\Delta\mathbf{U}_h+(\lambda+\mu)\mathbf{grad}(\mathrm{div}(\mathbf{U}_h))\big|^2\omega_T^{\alpha}\\
&= \int_T \big[\mathbf{f}_T+\mu\Delta\mathbf{U}_h+(\lambda+\mu)\mathbf{grad}(\mathrm{div}(\mathbf{U}_h))\big]^{\mathrm{T}}\mathbf{\Psi}_T\\
&= \int_T \omega_T^{\alpha/2}[\mathbf{f}_T-\mathbf{f}]^{\mathrm{T}}\mathbf{\Psi}_T\omega_T^{-\alpha/2}+\int_T \boldsymbol{\varepsilon}(\mathbf{U}-\mathbf{U}_h):\boldsymbol{\sigma}(\mathbf{\Psi}_T)\\
&\precsim \Big\{\|(\mathbf{f}_T-\mathbf{f})\omega_T^{\alpha/2}\|_{[\mathbb{L}_2(T)]^2}+\|\mathbf{U}-\mathbf{U}_h\|_{[\mathbb{H}^1(T)]^2}\frac{p^{(2-\alpha)}}{h(T)}\Big\}\times\\
&\quad \|\mathbf{\Psi}_T\omega^{-\alpha/2}\|_{[\mathbb{L}_2(T)]^2}.
\end{aligned}$$

The internal estimator verifies

$$\eta^{\mathbf{tri}}_{\alpha,T} = \frac{h(T)}{p}\|\mathbf{\Psi}_T\omega^{-\alpha/2}\|_{[\mathbb{L}_2(T)]^2} \tag{4.120}$$

$$\precsim \frac{h(T)}{p}\Big\{\frac{p^{(2-\alpha)}}{h(T)}\|\mathbf{U}-\mathbf{U}_h\|_{[\mathbb{H}^1(T)]^2}+\big\|(\mathbf{f}_T-\mathbf{f})\omega_T^{\alpha/2}\big\|_{[\mathbb{L}_2(T)]^2}\Big\} \tag{4.121}$$

$$\precsim p^{(1-\alpha)}\|\mathbf{U}-\mathbf{U}_h\|_{[\mathbb{H}^1(T)]^2}+\frac{h(T)}{p}\big\|(\mathbf{f}_T-\mathbf{f})\omega_T^{\alpha/2}\big\|_{[\mathbb{L}_2(T)]^2} \tag{4.122}$$

yielding (4.96). For an edge e incident upon $T_{(1,e)}$ and $T_{(2,e)}$, use $\mathcal{N}(e)=T_{(1,e)}\cup T_{(2,e)}$, define the vector-valued polynomial

$$\mathbf{R}_e := \boldsymbol{\sigma}(\mathbf{U}_h)_{|_{T_{(1,e)}}}\mathbf{n}(e)-\boldsymbol{\sigma}(\mathbf{U}_h)_{|_{T_{2,e}}}\mathbf{n}(e). \tag{4.123}$$

Let $\widetilde{\boldsymbol{\theta}}_e$ be the componentwise extension of $\mathbf{R}_e$ according to (4.92) on $\mathcal{N}(e)$ such that $\widetilde{\boldsymbol{\theta}}_e|_{\partial\mathcal{N}(e)}\equiv 0$ and $(\widetilde{\boldsymbol{\theta}}_e)|_e\equiv\mathbf{R}_e\omega_e^{\alpha}$. Define $\boldsymbol{\theta}_e:=\mathbf{R}_e\omega_e^{\alpha}$.

$$\int_e \mathbf{R}_e^{\mathrm{T}}\widetilde{\boldsymbol{\theta}}_e=\int_e|\mathbf{R}_e|^2\omega_e^{\alpha}=\int_e|\boldsymbol{\theta}_e|^2\omega_e^{-\alpha}=\|\boldsymbol{\theta}_e\omega_e^{-\alpha/2}\|^2_{[\mathbb{L}_2(e)]^2}. \tag{4.124}$$

On the other hand, one has

$$\int_e \mathbf{R}_e^{\mathrm{T}}\widetilde{\boldsymbol{\theta}}_e=\int_e(\boldsymbol{\sigma}(\mathbf{U}_h)_{|_{T_{(1,e)}}}\mathbf{n}(e))^{\mathrm{T}}\widetilde{\boldsymbol{\theta}}_e-\int_e(\boldsymbol{\sigma}(\mathbf{U}_h)_{|_{T_{(2,e)}}}\mathbf{n}(e))^{\mathrm{T}}\widetilde{\boldsymbol{\theta}}_e. \tag{4.125}$$

According to the first Green identity where the normal vector $\mathbf{n}(e)$ is supposed to be from $T_{(1,e)}$ toward $T_{(2,e)}$,

$$\begin{aligned}
\int_e(\boldsymbol{\sigma}(\mathbf{U}_h)_{|_{T_{(1,e)}}}\mathbf{n}(e))^{\mathrm{T}}\widetilde{\boldsymbol{\theta}}_e &= \int_{T_{(1,e)}}\boldsymbol{\varepsilon}(\mathbf{U}_h):\boldsymbol{\sigma}(\widetilde{\boldsymbol{\theta}}_e)+ &(4.126)\\
&\quad \int_{T_{(1,e)}}\{\mu\Delta\mathbf{U}_h+(\mu+\lambda)\mathbf{grad}(\mathrm{div}(\mathbf{U}_h))\}^{\mathrm{T}}\widetilde{\boldsymbol{\theta}}_e. &(4.127)
\end{aligned}$$

A similar equality with opposite sign is verified on $T_{2,e}$. Hence, by proceeding similarly for $\mathbf{U}$, one obtains

$$\begin{aligned}\int_e \mathbf{R}_e^{\mathrm{T}}\widetilde{\boldsymbol{\theta}}_e &= \int_{\mathcal{N}(e)} \boldsymbol{\varepsilon}(\mathbf{U}_h-\mathbf{U}):\boldsymbol{\sigma}(\widetilde{\boldsymbol{\theta}}_e)+\\ &\quad \int_{\mathcal{N}(e)} \{\mathbf{f}+\mu\Delta\mathbf{U}_h+(\mu+\lambda)\mathbf{grad}(\operatorname{div}\mathbf{U}_h)\}^{\mathrm{T}}\widetilde{\boldsymbol{\theta}}_e\\ &\leq \Big[\int_{\mathcal{N}(e)} \boldsymbol{\varepsilon}(\mathbf{U}_h-\mathbf{U}):\boldsymbol{\sigma}(\mathbf{U}_h-\mathbf{U})\Big]^{1/2}\Big[\int_{\mathcal{N}(e)} \boldsymbol{\varepsilon}(\widetilde{\boldsymbol{\theta}}_e):\boldsymbol{\sigma}(\widetilde{\boldsymbol{\theta}}_e)\Big]^{1/2}+\\ &\quad \big\|\mathbf{f}+\mu\Delta\mathbf{U}_h+(\mu+\lambda)\mathbf{grad}(\operatorname{div}\mathbf{U}_h)\big\|_{[\mathbb{L}_2(\mathcal{N}(e))]^2}\big\|\widetilde{\boldsymbol{\theta}}_e\big\|_{[\mathbb{L}_2(\mathcal{N}(e))]^2}\\ &\precsim \|\mathbf{U}-\mathbf{U}_h\|_{[\mathbb{H}^1(\mathcal{N}(e))]^2}\|\widetilde{\boldsymbol{\theta}}_e\|_{[\mathbb{H}^1(\mathcal{N}(e))]^2}+\\ &\quad \big\|\mathbf{f}+\mu\Delta\mathbf{U}_h+(\mu+\lambda)\mathbf{grad}(\operatorname{div}\mathbf{U}_h)\big\|_{[\mathbb{L}_2(\mathcal{N}(e))]^2}\big\|\widetilde{\boldsymbol{\theta}}_e\big\|_{[\mathbb{L}_2(\mathcal{N}(e))]^2}.\end{aligned}$$

According to the properties (4.93) and (4.94) of the extension operator componentwise,

$$\|\widetilde{\boldsymbol{\theta}}_e\|^2_{[\mathbb{L}_2(T_{i,e})]^2} \precsim h(T_{i,e})\gamma\|\boldsymbol{\theta}_e\omega_e^{-\alpha/2}\|^2_{[\mathbb{L}_2(e)]^2} \tag{4.128}$$

$$|\widetilde{\boldsymbol{\theta}}_e|^2_{[\mathbb{H}^1(T_{i,e})]^2} \precsim \frac{1}{h(T_{i,e})}(\gamma p^{2(2-\alpha)}+\gamma^{-1})\|\boldsymbol{\theta}_e\omega_e^{-\alpha/2}\|^2_{[\mathbb{L}_2(e)]^2}. \tag{4.129}$$

By using (4.124) and the above two estimates, obtain

$$\begin{aligned}\|\boldsymbol{\theta}_e\omega_e^{-\alpha/2}\|_{[\mathbb{L}_2(e)]^2} &\leq \|\mathbf{U}-\mathbf{U}_h\|_{[\mathbb{H}^1(\mathcal{N}(e))]^2}\Big[\sum_{T\in\omega(e)}\frac{1}{h(T)}(\gamma p^{2(2-\alpha)}+\gamma^{-1})\Big]^{1/2}+\\ &\quad \big\|\mathbf{f}+\mu\Delta\mathbf{U}_h+(\mu+\lambda)\mathbf{grad}(\operatorname{div}\mathbf{U}_h)\big\|_{[\mathbb{L}_2(\mathcal{N}(e))]^2}\sum_{T\in\omega(e)}\sqrt{h(T)\gamma}.\end{aligned}$$

Since the edge estimator $\eta_{\alpha,e}^{\mathbf{edg}}=\sqrt{h(e)/(2p)}\|\boldsymbol{\theta}_e\omega_e^{-\alpha/2}\|_{[\mathbb{L}_2(e)]^2}$ and by using $h(e)\simeq h(T)$ for $T\in\mathcal{N}(e)$, obtain

$$\eta_{\alpha,e}^{\mathbf{edg}}\leq C_p\|\mathbf{U}-\mathbf{U}_h\|_{[\mathbb{H}^1(\mathcal{N}(e))]^2}+\sum_{T\in\mathcal{N}(e)}\frac{h(T)}{\sqrt{p}}\mathrm{OSC}(\mathbf{f},\mathbf{f}_h,T) \tag{4.130}$$

which provides (4.98).

Reliability: For any $\mathbf{W} \in [H_0^1(\mathbf{\Omega})]^2$

$$\begin{aligned} R &:= \int_{\mathbf{\Omega}} \boldsymbol{\varepsilon}(\mathbf{U}-\mathbf{U}_h) : \boldsymbol{\sigma}(\mathbf{W}) = \int_{\mathbf{\Omega}} \mathbf{f}^{\mathrm{T}}\mathbf{W} + \sum_{T\in\mathbb{M}_h(\mathbf{\Omega})} \Big\{ \int_{\partial T} -[\boldsymbol{\sigma}(\mathbf{U}_h)\mathbf{n}]^T\mathbf{W} \\ &\quad + \int_T [\mu\Delta\mathbf{U}_h + (\lambda+\mu)\mathbf{grad}(\mathrm{div}\mathbf{U}_h)]^{\mathrm{T}}\mathbf{W} \\ &= \sum_{T\in\mathbb{M}_h(\mathbf{\Omega})} \int_T [\mathbf{f} + \mu\Delta\mathbf{U}_h + (\lambda+\mu)\mathbf{grad}(\mathrm{div}\mathbf{U}_h)]^{\mathrm{T}}\mathbf{W} + \\ &\quad \sum_{e\in\mathbb{E}_h(\mathbf{\Omega})} \int_e \Big[\boldsymbol{\sigma}(\mathbf{U}_h)|_{T_{(1,e)}}\mathbf{n}(e) - \boldsymbol{\sigma}(\mathbf{U}_h)|_{T_{(2,e)}}\mathbf{n}(e)\Big]^T\mathbf{W}. \end{aligned}$$

In particular, for $\mathbf{W} = (\mathbf{U}-\mathbf{U}_h) - \mathbf{I}_{h,p}(\mathbf{U}-\mathbf{U}_h)$ where $\mathbf{I}_{h,p}$ is the componentwise Clément interpolant [19, 20], one has in term of the energy norm (2.15)

$$\begin{aligned} \|\!|\mathbf{U}-\mathbf{U}_h|\!\|_E^2 &\precsim \sum_{T\in\mathbb{M}_h(\mathbf{\Omega})} \|\mathbf{f} + \mu\Delta\mathbf{U}_h + (\lambda+\mu)\mathbf{grad}(\mathrm{div}\mathbf{U}_h)\|_{[\mathbb{L}_2(T)]^2}\|\mathbf{W}\|_{[\mathbb{L}_2(T)]^2} + \\ &\quad \sum_{e\in\mathbb{E}_h(\mathbf{\Omega})} \|\boldsymbol{\sigma}(\mathbf{U}_h)|_{T_{(1,e)}}\mathbf{n}(e) - \boldsymbol{\sigma}(\mathbf{U}_h)|_{T_{(2,e)}}\mathbf{n}(e)\|_{[\mathbb{L}_2(e)]^2}\|\mathbf{W}\|_{[\mathbb{L}_2(e)]^2}. \end{aligned}$$

By using the properties of $\mathbf{I}_{h,p}$, one deduces

$$\|\mathbf{W}\|_{[\mathbb{L}_2(T)]^2} \leq \frac{h(T)}{p}\|\mathbf{U}-\mathbf{U}_h\|_{[\mathbb{H}^1(\mathcal{N}(T))]^2} \tag{4.131}$$

$$\|\mathbf{W}\|_{[\mathbb{L}_2(e)]^2} \leq \sqrt{\frac{h(e)}{p}}\|\mathbf{U}-\mathbf{U}_h\|_{[\mathbb{H}^1(\mathcal{N}(e))]^2}. \tag{4.132}$$

A combination of the fact that both $\mathcal{N}(T)$ and $\mathcal{N}(e)$ contain a few number of elements, Cauchy-Schwarz and the equivalence (2.16) yields

$$\begin{aligned} \|\mathbf{U}-\mathbf{U}_h\|_{[\mathbb{H}^1(\mathbf{\Omega})]^2} &\precsim \sum_{T\in\mathbb{M}_h(\mathbf{\Omega})} \frac{h(T)}{p}\|\mathbf{f}-\mathbf{f}_T\|_{[\mathbb{L}_2(T)]^2} + \\ &\quad \sum_{T\in\mathbb{M}_h(\mathbf{\Omega})} \Big\{ \frac{h^2(T)}{p^2}\|\mathbf{f}_T + \mu\Delta\mathbf{U}_h + (\lambda+\mu)\mathbf{grad}(\mathrm{div}\mathbf{U}_h)\|^2_{[\mathbb{L}_2(T)]^2} + \\ &\quad \sum_{e\subset T, e\in\mathbb{E}_h(\mathbf{\Omega})} \frac{h(e)}{p}\|\boldsymbol{\sigma}(\mathbf{U}_h)|_{T_{(1,e)}}\mathbf{n}(e) - \boldsymbol{\sigma}(\mathbf{U}_h)|_{T_{(2,e)}}\mathbf{n}(e)\|^2_{[\mathbb{L}_2(e)]^2} \Big\}^{1/2} \end{aligned}$$

which provides the result for the weight-free case ($\omega_T^\alpha \equiv 1$). As for the weight-based case ($\alpha \neq 0$), apply the polynomial inverse estimate (3.34) componentwise to the vector valued polynomial $\boldsymbol{\pi}_p = \mathbf{f}_T + \mu\Delta\mathbf{U}_h + (\lambda+\mu)\mathbf{grad}(\mathrm{div}\mathbf{U}_h)$ to obtain

$$\|\boldsymbol{\pi}_p\|_{[\mathbb{L}_2(T)]^2} \precsim p^\alpha \|\boldsymbol{\pi}_p\omega_T^{\alpha/2}\|_{[\mathbb{L}_2(T)]^2} \tag{4.133}$$

and a similar estimate for $\boldsymbol{\pi}_p = \boldsymbol{\sigma}(\mathbf{U}_h)|_{T_{(1,e)}}\mathbf{n}(e) - \boldsymbol{\sigma}(\mathbf{U}_h)|_{T_{(2,e)}}\mathbf{n}(e)$

$$\|\mathbf{U}-\mathbf{U}_h\|_{[\mathbb{H}^1(\boldsymbol{\Omega})]^2} \lesssim C_p \sum_{T\in\mathbb{M}_h(\boldsymbol{\Omega})} \Big[(\eta_{\alpha,T}^{\mathbf{tri}})^2 + \sum_{e\subset\partial T,\, e\in\mathbb{E}_h^{\mathbf{int}}} (\eta_{\alpha,e}^{\mathbf{edg}})^2\Big]^{1/2} + \tag{4.134}$$

$$\sum_{T\in\mathbb{M}_h(\boldsymbol{\Omega})} \frac{h(T)}{p}\|\mathbf{f}-\mathbf{f}_T\|_{[\mathbb{L}_2(T)]^2}. \tag{4.135}$$

■

5. Software and numerical results

In this section which is subdivided into two parts, we want to describe the numerical implementation of the former method. First, we concentrate on the description of the software and its numerical outcomes. The second part describes the comparison between the exact FEM-accuracy and the a-posteriori error estimates.

5.1. **Software and exact accuracies.** The software is implemented by using a combination of C functions and C++ classes. Some LAPACK and BLAS routines are used sometimes to perform various linear algebraic operations. The software which functions in both 2D and 3D was initially inspired from the MATLAB piecewise linear implementation [3] and then it was generalized to higher order FEM. Our first test consists in computing the accuracies $\big\|\mathbf{U}-\mathbf{U}_h\big\|_{[\mathbb{L}_2(\boldsymbol{\Omega})]^2}$, $\big\|\boldsymbol{\varepsilon}-\boldsymbol{\varepsilon}_h\big\|_{[\mathbb{L}_2(\boldsymbol{\Omega})]^{2\times 2}}$, $\big\|\boldsymbol{\sigma}-\boldsymbol{\sigma}_h\big\|_{[\mathbb{L}_2(\boldsymbol{\Omega})]^{2\times 2}}$. The exact solution is $\mathbf{U}(\mathbf{x}) = \big[1.5\sin(2\pi x_1)\,\sin(2\pi x_2),\, -0.75\sin(2\pi x_1)\,\sin(2\pi x_2)\big]^{\mathrm{T}}$ in $\boldsymbol{\Omega} = [0,1]\times[0,1]$. The expressions of the right hand side $\mathbf{f}$, the exact strain tensor $\boldsymbol{\varepsilon}$ as well as the stress tensor $\boldsymbol{\sigma}$ are computed according to (2.4), (2.5) and (2.9).

Since the FEM-level is used extensively, we introduce it very rapidly. For a given mesh $\mathbb{M}_h(\boldsymbol{\Omega})$ on the current level ℓ, another mesh on the next level $(\ell+1)$ is constructed by subdividing every edge in the middle of which one inserts a new node. Therefore, that corresponds to a global uniform refinement where every element is locally subdivided. Only the mesh on the coarsest level (level $\ell = 1$ in our entire study) is provided. For the next case, the coarse mesh is a simple tensor product mesh with step sizes $h_1 = 1/10$, $h_2 = 1/10$ on the horizontal and the vertical axes corresponding to $h = \sqrt{h_1^2+h_2^2}$. One level incrementation amounts to reducing the mesh size from h to $h/2$. The results are collected in Table 5.1 where we use polynomial degrees one till three. For each polynomial degree, the FEM-level ranges from one to four while the Lamé constants are $(\lambda,\mu) = (0.3, 0.75)$.

The ratio ρ_p between the accuracy on level ℓ and the accuracy on the preceding level $\ell-1$ for the polynomial degree p will be termed contraction. For the linear case where the polynomial degree $p = 1$, one has the average contractions of $\rho_1(\mathbf{U}) = 3.79$, $\rho_1(\boldsymbol{\varepsilon}) = 1.96$

p	Lev	Displac.	Strain	Stress
1	1	$\begin{bmatrix} 1.256E-01 \\ 9.067E-02 \end{bmatrix}$	$\begin{bmatrix} 1.595E+00 & 9.309E-01 \\ 9.309E-01 & 8.310E-01 \end{bmatrix}$	$\begin{bmatrix} 2.899E+00 & 1.396E+00 \\ 1.396E+00 & 1.599E+00 \end{bmatrix}$
	2	$\begin{bmatrix} 3.501E-02 \\ 2.598E-02 \end{bmatrix}$	$\begin{bmatrix} 8.167E-01 & 5.022E-01 \\ 5.022E-01 & 4.143E-01 \end{bmatrix}$	$\begin{bmatrix} 1.505E+00 & 7.533E-01 \\ 7.533E-01 & 8.399E-01 \end{bmatrix}$
	3	$\begin{bmatrix} 9.027E-03 \\ 6.751E-03 \end{bmatrix}$	$\begin{bmatrix} 4.105E-01 & 2.567E-01 \\ 2.567E-01 & 2.060E-01 \end{bmatrix}$	$\begin{bmatrix} 7.603E-01 & 3.851E-01 \\ 3.851E-01 & 4.254E-01 \end{bmatrix}$
	4	$\begin{bmatrix} 2.274E-03 \\ 1.704E-03 \end{bmatrix}$	$\begin{bmatrix} 2.055E-01 & 1.291E-01 \\ 1.291E-01 & 1.028E-01 \end{bmatrix}$	$\begin{bmatrix} 3.811E-01 & 1.936E-01 \\ 1.936E-01 & 2.134E-01 \end{bmatrix}$
2	1	$\begin{bmatrix} 4.917E-03 \\ 2.901E-03 \end{bmatrix}$	$\begin{bmatrix} 2.156E-01 & 1.314E-01 \\ 1.314E-01 & 1.073E-01 \end{bmatrix}$	$\begin{bmatrix} 3.932E-01 & 1.972E-01 \\ 1.972E-01 & 2.110E-01 \end{bmatrix}$
	2	$\begin{bmatrix} 5.911E-04 \\ 3.147E-04 \end{bmatrix}$	$\begin{bmatrix} 5.586E-02 & 3.390E-02 \\ 3.390E-02 & 2.788E-02 \end{bmatrix}$	$\begin{bmatrix} 1.024E-01 & 5.086E-02 \\ 5.086E-02 & 5.581E-02 \end{bmatrix}$
	3	$\begin{bmatrix} 7.287E-05 \\ 3.710E-05 \end{bmatrix}$	$\begin{bmatrix} 1.410E-02 & 8.541E-03 \\ 8.541E-03 & 7.049E-03 \end{bmatrix}$	$\begin{bmatrix} 2.590E-02 & 1.281E-02 \\ 1.281E-02 & 1.418E-02 \end{bmatrix}$
	4	$\begin{bmatrix} 9.075E-06 \\ 4.559E-06 \end{bmatrix}$	$\begin{bmatrix} 3.535E-03 & 2.139E-03 \\ 2.139E-03 & 1.767E-03 \end{bmatrix}$	$\begin{bmatrix} 6.497E-03 & 3.209E-03 \\ 3.209E-03 & 3.560E-03 \end{bmatrix}$
3	1	$\begin{bmatrix} 3.144E-04 \\ 1.679E-04 \end{bmatrix}$	$\begin{bmatrix} 1.945E-02 & 1.034E-02 \\ 1.034E-02 & 9.865E-03 \end{bmatrix}$	$\begin{bmatrix} 3.456E-02 & 1.552E-02 \\ 1.552E-02 & 1.758E-02 \end{bmatrix}$
	2	$\begin{bmatrix} 1.849E-05 \\ 9.464E-06 \end{bmatrix}$	$\begin{bmatrix} 2.445E-03 & 1.285E-03 \\ 1.285E-03 & 1.236E-03 \end{bmatrix}$	$\begin{bmatrix} 4.353E-03 & 1.927E-03 \\ 1.927E-03 & 2.218E-03 \end{bmatrix}$
	3	$\begin{bmatrix} 1.127E-06 \\ 5.678E-07 \end{bmatrix}$	$\begin{bmatrix} 3.057E-04 & 1.597E-04 \\ 1.597E-04 & 1.543E-04 \end{bmatrix}$	$\begin{bmatrix} 5.443E-04 & 2.396E-04 \\ 2.396E-04 & 2.774E-04 \end{bmatrix}$
	4	$\begin{bmatrix} 7.139E-08 \\ 4.496E-08 \end{bmatrix}$	$\begin{bmatrix} 3.819E-05 & 1.991E-05 \\ 1.991E-05 & 1.927E-05 \end{bmatrix}$	$\begin{bmatrix} 6.800E-05 & 2.987E-05 \\ 2.987E-05 & 3.464E-05 \end{bmatrix}$

TABLE 5.1. $\mathbb{L}_2$-accuracies of the elastic values for polynomial degrees $p = 1, 2, 3$.

and $\rho_1(\boldsymbol{\sigma}) = 1.94$ for the displacement, strain and stress respectively. The average contraction ratios for the quadratic case are $\rho_2(\mathbf{U}) = 8.38$, $\rho_2(\boldsymbol{\varepsilon}) = 3.94$ and $\rho_2(\boldsymbol{\sigma}) = 3.93$ while those for the cubic case are $\rho_3(\mathbf{U}) = 16.04$, $\rho_3(\boldsymbol{\varepsilon}) = 8.01$ and $\rho_3(\boldsymbol{\sigma}) = 8.01$.

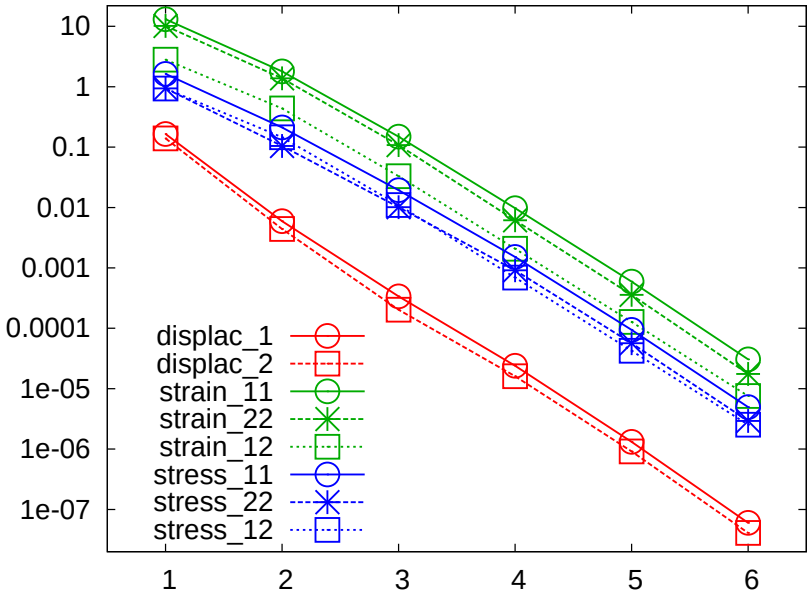

FIGURE 2. Accuracies of the displacement, strain and stress in function of increasing polynomial degree $p = 1, ..., 6$.

Our next test consists in investigating the software for the case of increasing polynomial degree. The corresponding results are collected in Figure 2 where we consider the $\mathbb{L}_2$-accuracy for the displacement, strain and stress: $\|U_1 - U_{1,h}\|_{\mathbb{L}_2(\mathbf{\Omega})}$, $\|U_2 - U_{2,h}\|_{\mathbb{L}_2(\mathbf{\Omega})}$, $\|\varepsilon_{11} - \varepsilon_{11,h}\|_{\mathbb{L}_2(\mathbf{\Omega})}$, $\|\varepsilon_{22} - \varepsilon_{22,h}\|_{\mathbb{L}_2(\mathbf{\Omega})}$, $\|\varepsilon_{12} - \varepsilon_{12,h}\|_{\mathbb{L}_2(\mathbf{\Omega})}$, $\|\sigma_{11} - \sigma_{11,h}\|_{\mathbb{L}_2(\mathbf{\Omega})}$, $\|\sigma_{22} - \sigma_{22,h}\|_{\mathbb{L}_2(\mathbf{\Omega})}$ and $\|\sigma_{12} - \sigma_{12,h}\|_{\mathbb{L}_2(\mathbf{\Omega})}$. The strain component ε_{21} and the stress component σ_{21} are omitted because they are the same as ε_{12}, σ_{12} respectively. The polynomial degree ranges from one to six and the Lamé coefficients are $(\lambda, \mu) = (5, 1.5)$. Since the vertical axis is logarithmically scaled, this experiment highlights that all the accuracies decrease exponentially proportional with the polynomial degree. Thus, our practical software is in accordance with the well known FEM-accuracy with respect to the polynomial degree. Both the accuracies of the strain and stress are a little worse than that of the displacement because the expressions of the stress and the strain involve partial derivatives of the displacements as appearing in (2.4) and (2.5). A result of the effect of static computation using vertical gravity load $\mathbf{f} = [0, -1]^T$ due to the objects own weight is depicted in Figure 3. Another computation using zero body force where an object is fixed on one end while it is pulled on the other is also shown in the same figure. The object consists of a rectangle admitting 3 circular perforations. Since the displacement is tiny, it is magnified for visualization purpose. Figure 4 depicts the distribution of the Tresca stress of an elastic object under some elastic constraints.

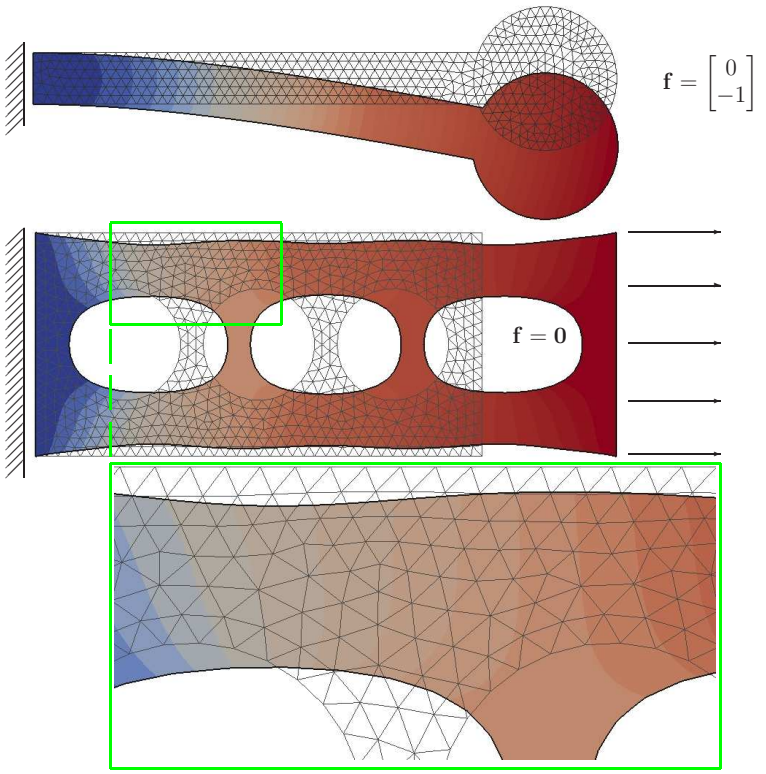

FIGURE 3. Top: deformation caused by a vertical downward gravity. Middle: magnified deformation by pulling. Bottom: zoom of the marked area.

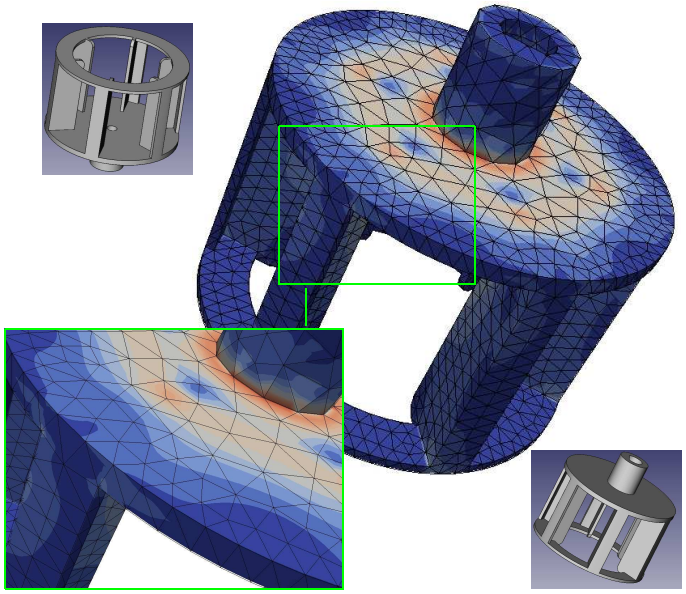

FIGURE 4. Tresca stress distribution on a CAD object under elasticity constraints

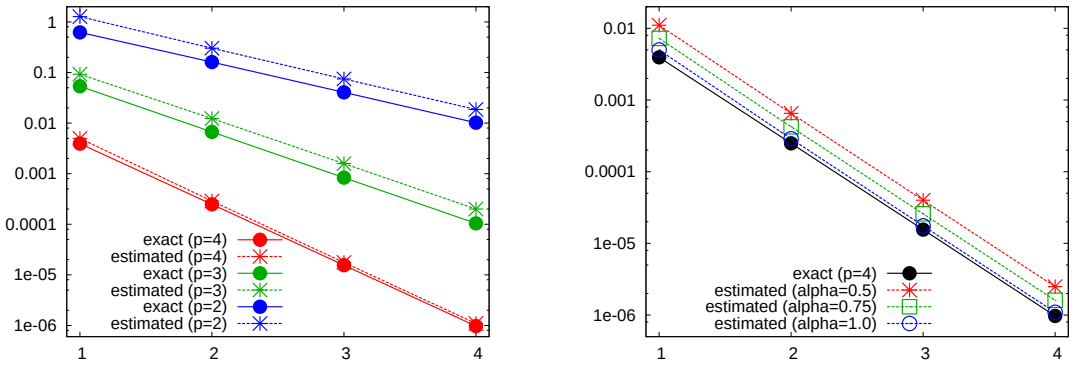

(a) (b)

FIGURE 5. In function of the levels: (a)several polynomial degrees p, (b)several weight exponents α.

5.2. **Practical a-posteriori estimates.** Now that we have gained insight about the a-priori accuracy, we want to turn our attention to the a-posteriori estimator η_α. The principal role of an a-posteriori error estimator is twofold. For one, it serves as gaining some idea of whether to continue or to abort a simulation. The computation is aborted when the desired precision is provided by the estimator. Since the exact solution u is not known for real applications, an estimator is needed. A further purpose of the error estimator is to identify the regions within the domain $\mathbf{\Omega}$ where the precision is unsatisfactory. Mesh refinements are therefore applied at those regions to improve the local precision. The proposed estimator can be used for both purposes but we have currently only the first utility in our computer implementation. According to the proposed theory, it is sufficient to conduct a comparison between the $\mathbb{H}^1$-error and the error estimator η_α. We examine the agreements between the exact precision $\|\mathbf{U}-\mathbf{U}_h\|_{[\mathbb{H}^1(\mathbf{\Omega})]^2}$ and the estimated precision η_α when the FEM-level increases. We perform two sets of tests whose outcomes are displayed in Figure 5(a) and Figure 5(b). The first test compares the exact precision and the estimated precision for a fixed polynomial degree which ranges from two to four. The considered value of the parameter α is 0.25 while the FEM-level is allowed to vary from one to four. We observe that the proposed estimators capture the exact precision up to some constant factors. In fact, the decrease of the exact and the estimated precisions follow the same pace as the FEM-level increases. The second test consists in considering several values of the parameter α for a fixed value of the polynomial degree which is taken to be $p=4$. The considered values are $\alpha=0.5$, $\alpha=0.75$ and $\alpha=1.0$. For all values of α, the results in Figure 5 highlight that the estimator η_α provides an efficient estimation of the exact

precision as predicted theoretically. In addition, the decrease of the exact precision agrees well with the decrease of the error estimator η_α as the FEM-levels grow. In fact, the estimations by η_α are somewhat influenced by the values of the chosen α. Nonetheless, the values of η_α are comparatively of the same order up to some constant scaling factors. At this point, we do no know exactly which value of the parameter α to be chosen. There is no mathematical study to adjust it, let alone to find its optimal value. It is conceivable to choose the value of α adaptively but we do not have that utility at the time being. All values of α in $[0, 1]$ provide an efficient a-posteriori error estimator.

Conclusion and future works

Some polynomial inverse estimates have been considered for the use in the a-posteriori error estimators of a problem stemming from elastostatic. We considered the case where the polynomial degree p is fixed in the entire mesh. The method turns out to be efficient and reliable. That can be very well observed for various values of the fixed polynomial degree p. That highlights that using the estimator makes sense to evaluate the desired precision. Our ongoing and future works are as follows. The case where the constants C_p in the estimates are completely free of the polynomial degree appears to be still an open problem. Having such estimates is important when one allows variable polynomial degrees $p(T)$ in different elements of the same mesh. Another valuable theoretical aspect might be to consider the dependence on the parameters (λ, μ) in the bounding of the estimators especially in the case approaching incompressible elasticity or in the case the domain $\mathbf{\Omega}$ is composed of many subdomains $\mathbf{\Omega}_i$, each having its own (λ_i, μ_i). In term of computer implementation, we might improve our CAD integration of static computation which is for the time being not completely automatized. In addition, slow execution is observed in the estimators where integrals are computed by quadratures whose number becomes very large when the polynomial degree is high. Since the expression of the weighted integrands of the estimator is now explicitly known, it is conceivable to search for an explicit formula to evaluate the integrals analytically.

References

[1] V. ADAMS, A. ASKENAZI, *Building better products with finite element analysis*, On-Word Press, 1999.

[2] M. AINSWORTH, T. ODEN, *A Posteriori error estimators for the Stokes and Oseen equations*, SIAM J. Numer. Anal. **34**, pp. 228–245, 1997.

[3] J. ALBERTY, C. CARTENSEN, S. FUNKEN, R. KLOSE, *Matlab implementation of the finite element method in elasticity*, Computing **69**, pp. 239-263, 2002.

[4] I. BABUSKA, M. SURI, *Locking effects in the finite element approximation of elasticity problems*, Numerische Mathematik **62**, No. 1, pp. 439–463, 1992.

[5] I. BABUSKA, M. SURI, *The hp-version of the finite element method with quasiuniform meshes*, ESAIM: Mathematical Modelling and Numerical Analysis **21**, No. 2, pp. 199–238, 1987.

[6] R. BANK, A. SHERMAN, A. WEISER, *Some refinement algorithms and data structures for regular local mesh refinement*, In Scientific Computing, R. Stepleman et al. **44**, IMACS North-Holland, Amsterdam. pp. 3–17, 1983.

[7] C. BERNARDI, *Indicateurs d'erreur en h-N version des éléments spectraux*, Modélisation Mathématique et Analyse Numérique **30**, No. 1, pp. 1–38, 1996.

[8] C. BERNARDI, M. DAUGE, Y. MADAY, *Polynomials in the Sobolev world*, Preprint of the Laboratoire Jacques-Louis Lions, No. R03038, 2003.

[9] C. BERNARDI, Y. MADAY, *Polynomial interpolation results in Sobolev spaces*. Journal of Computational and Applied Mathematics **43**, No. 1–2, pp. 53–80, 1992.

[10] C. CARSTENSEN, S. BARTELS, *Each averaging technique yields reliable a-posteriori error control in FEM on unstructured grids. Part I: low order conforming, nonconforming, and mixed FEM*. Mathematics of Computation **71**, No. 239, pp. 945-969, 2002.

[11] E. CREUSÉ, G. KUNERT, S. NICAISE, *A posteriori error estimation for the Stokes problem: anisotropic and isotropic discretizations*, Mathematical Models and Methods in Applied Sciences **14**, No. 9, pp. 1297–1341, 2004.

[12] C. DIEDRICH, D. DIJKSTRA, J. HAMAEKERS, B. HENNINGER, M. RANDRIANARIVONY, *A finite element study on the effect of curvature on the reinforcement of matrices by randomly distributed and curved nanotubes*, Journal of Computational and Theoretical Nanoscience **12**, pp. 2108–2116, 2015.

[13] M. DOBROWOLSKI, S. GRÄF, C. PFLAUM, *A Posteriori error estimators in the finite element method on anisotropic meshes*, ETNA **8**, pp. 36–45, 1999.

[14] J. JOU, J. LIU, *An a posteriori finite element analysis for the Stokes equations*, J. Comput. Appl. Math. **114**, pp. 333-343, 2000.

[15] H. HARBRECHT, M. RANDRIANARIVONY, *From Computer Aided Design to wavelet BEM*, Comput. Vis. Sci. **13**, No. 2, pp. 69–82 (2010).

[16] G. KUNERT, R. VERFÜRTH, *Edge residuals dominate a posteriori error estimates for linear finite element methods on anisotropic triangular and tetrahedral meshes*, Numer. Math. **86**, pp. 283-303, 2000.

[17] Y. MADAY. *Analysis of spectral projectors in one-dimensional domains*, Mathematics of Computation **55**, No. 192, pp. 537–562, 1990.

[18] W. MCLEAN, *Strongly elliptic systems and boundary integral equations*, Cambridge University Press, Cambridge (2000).

[19] J. MELENK, B. WOHLMUTH, *On residual-based a posteriori error estimation in hp-FEM*, Adv. Comput. Math. **15**, No. 1–4, pp. 311-331, 2002.

[20] J. MELENK, *hp-interpolation of non-smooth functions*, SIAM J. Numer. Anal. **43**, pp. 127–155, 2005.

[21] M. RANDRIANARIVONY, G. BRUNNETT, *Preparation of CAD and molecular surfaces for meshfree solvers*, Lecture Notes in Computational Science and Engineering **65**, pp. 231–245, 2008.

[22] M. RANDRIANARIVONY, *Harmonic variation of edge size in meshing CAD geometries from IGES format*. Lecture Notes in Computer Science **5102**, pp. 56–65, 2008.

[23] M. RANDRIANARIVONY, *Anisotropic finite elements for the Stokes problem: a-posteriori error estimator and adaptive mesh*, Journal of Computational and Applied Mathematics **169**, No. 2, pp. 255–275, 2004.

[24] M. RANDRIANARIVONY, *Geometric processing of CAD data and meshes as input of integral equation solvers*, Ph.D. thesis, Technical University of Chemnitz, Germany, 2006.

[25] M. RANDRIANARIVONY, *On global continuity of Coons mappings in patching CAD surfaces*, Comput.-Aided Design **41**, No. 11, pp. 782–791, 2009.

[26] M. RANDRIANARIVONY, *Domain decomposition for wavelet single layer on geometries with patches*, Applied Mathematics **7**, No. 15, pp. 1798–1823, 2016.

[27] M. RANDRIANARIVONY, *Stability of mixed finite element methods on anisotropic meshes*, Master's thesis, Faculty of mathematics, Technische Universität Chemnitz, 2001.

[28] M. RANDRIANARIVONY, *Multiwavelet Boundary Element Method for cavities admitting many NURBS patches*, Modeling and Numerical Simulation **6**, No. 4, pp. 69–93, 2016.

[29] M. RANDRIANARIVONY, *Analytical Polarizable Continuum Model for Wavelets on NURBS Patches*, Applied Mathematics **8**, No. 8, pp. 1045–1073, 2017.

[30] K. SIEBERT, *An a posteriori error estimator for anisotropic refinement*, Numer. Math. **73**, No.3, pp. 373–398, 1996.

[31] M. SURI, *The p-version of the finite element method for elliptic equations of order* $2l$, Modélisation mathématique et analyse numérique **24**, No. 2, pp. 265–304, 1990.

[32] M. SURI, *The p and hp finite element method for problems on thin domains*, Journal of Computational and Applied Mathematics **128**, pp. 235-260, 2001.

[33] R. VERFÜRTH, *A-posteriori error estimation and adaptive mesh refinement techniques*, Journal of Computational and Applied Mathematics **50**, pp. 67–83, 1994.

[34] R. VERFÜRTH, *A-posteriori error estimators for the Stokes equations*, Numer. Math. **55**, pp. 309-325, 1989.

[35] R. VERFÜRTH, *A-posteriori error estimators for the Stokes equations II: nonconforming discretizations*, Numer. Math. **60**, pp. 235-249, 1991.

[36] M. VOGELIUS, *An analysis of the p-version of the finite element method for nearly incompressible materials. Uniformly valid, optimal error estimates*, Numerische Mathematik **41**, No. 1, pp. 39–53, 1983.

[37] B. WOHLMUTH, *A residual based error estimator for mortar finite element discretization*, Numer. Math. **84**, pp. 143–171, 1999.